NMR Characteristics of Possible Oxygen Sites in Aluminosilicate Glasses and Melts: An ab Initio Study

Xianyu Xue* and Masami Kanzaki

Institute for Study of the Earth's Interior, Okayama University, Misasa, Tottori, 682-0193 Japan

Received: June 24, 1999; In Final Form: October 5, 1999

Ab initio molecular orbital calculations have been carried out for silicate, aluminosilicate, and aluminate clusters in order to study the NMR characteristics of oxygen sites that are possibly present in the structure of aluminosilicate glasses and melts. Of particular interest are the different types of bridging oxygens (oxygens bonded to two tetrahedrally coordinated Si and/or Al) and tricluster oxygens (oxygens linked to three tetrahedrally coordinated Si and/or Al). The calculated values for the ^{17}O quadrupolar coupling constants (QCC) of Si−O−Si, Si−O−Al, and Al−O−Al bridging oxygens agree reasonably well with experimental NMR data for similar oxygen sites in crystalline silicates, aluminosilicates, or aluminates, and do not show significant dependence on the basis set and theory (Hartree−Fock vs density functional theory) of calculations. The calculated values for the ^{17}O isotropic chemical shift (δ_i^O), on the other hand, show large dependence on the basis set and method of calculations, although the relative differences in δ_i^O for the clusters of interest do not vary as much. Our calculations indicate that bridging oxygens give progressively larger ^{17}O QCC and larger, but overlapping, δ_i^O from Al−O−Al to Si−O−Al to Si−O−Si. Coordination of Si−O−Al or Al−O−Al bridging oxygens to Ca^{2+}, a network-modifying cation, tends to decrease their ^{17}O QCC and increase their δ_i^O, consistent with experimental NMR data. Tricluster oxygens give progressively larger ^{17}O QCC and larger δ_i^O values from $O(Al_3)$, to $O(SiAl_2)$, to $O(Si_2Al)$, to $O(Si_3)$. The $O(Al_3)$ and $O(SiAl_2)$ tricluster oxygens have ^{17}O NMR characteristics overlapping with those of Si−O−Al bridging oxygens, and the $O(Si_2Al)$ tricluster oxygen overlapping with those of Si−O−Si bridging oxygens. Our calculations suggest that it may be difficult to distinguish $O(Al_3)$, $O(SiAl_2)$, or $O(Si_2Al)$ tricluster oxygens from bridging oxygens in aluminosilicate glasses on the basis of ^{17}O NMR data alone, although it should be possible to distinguish $O(Al_3)$ tricluster oxygen from Al−O−Al bridging oxygen in aluminates using ^{17}O NMR. The $O(Si_3)$ tricluster have larger ^{17}O QCC and larger δ_i^O values than all types of bridging oxygens and thus may be unambiguously identified on the basis of ^{17}O NMR data, if present in the structure of aluminosilicates or silicates.

Introduction

Aluminosilicate glasses and melts are of considerable interest to both materials sciences and Earth sciences because most of the synthetic glasses and natural magmas are of aluminosilicate compositions. Although the structures of aluminosilicate glasses and melts have been the subject of considerable spectroscopic studies, several controversial issues still remain. The structure and properties of aluminosilicate glasses and melts in the $M_xO-SiO_2-Al_2O_3$ system (where M_xO stands for network-modifying metal oxides, such as CaO, MgO, and Na_2O) at ambient pressure depend strongly on the M_xO/Al_2O_3 ratio. For systems with the M_xO/Al_2O_3 ratio greater than unity (peralkaline aluminosilicates), it is generally considered that both Si^{4+} and Al^{3+} assume tetrahedral coordination (Si^{IV} and Al^{IV}). The SiO_4 or AlO_4 tetrahedron, which constitutes the smallest structural units, shares each corner with another SiO_4 or AlO_4 tetrahedron, forming a three-dimensional tetrahedral network. The charge deficiency of Al^{3+} is compensated by the M cations. Any excess M cations over that required for charge balance are considered to play a network-modifying role to break up the network structure. From the prospect of oxygen environments, there are two types of oxygens in this structure model: bridging oxygen (BO) that bridges two SiO_4 or AlO_4 tetrahedra within the network and nonbridging oxygen (NBO) that links one SiO_4 or AlO_4 tetrahedron to one or more network-modifying M cations. The proportion of BO and NBO determines the degree of polymerization of the structure and controls to a large extent the properties (e.g., viscosity) of the glasses and melts. For systems with the $M_xO/Al_2O_3 = 1$ (tectosilicates), it has generally been accepted until recently that because the abundance of the M cation is exactly that required to balance the charge deficiency of Al^{IV}, the structure is fully polymerized with all oxygens being BOs.[1] This notion was generally supported by the observation that the melt viscosity reaches a maximum near the tectosilicate composition across the $M_xO-Al_2O_3$ join.[1] However, recent enhanced-precision viscosity data for melts in the $Na_2O-Al_2O_3-SiO_2$ system by Toplis et al.[2] suggested that the viscosity maximum actually deviates from the tectosilicate composition to the higher Al_2O_3 side. These authors inferred that this might be an indication that NBOs are still present in the melts of tectosilicate stoichiometry. More recently, Stebbins and Xu[3] reported the detection of about 5% NBO in an anorthite ($CaAl_2Si_2O_8$) glass (tectosilicate) using ^{17}O magic-angle spinning (MAS) and triple quantum (3Q) MAS NMR techniques. The presence of NBO in such a system, in the absence of higher coordination Al and Si as these authors have suggested, would require the concurrent occurrence of other types of oxygen sites that are linked to more than two SiO_4 or AlO_4 tetrahedra. Both

* Corresponding author. Phone: 81-858-43-3724. Fax: 81-858-43-2184. E-mail: xianyu@dbmac1.misasa.okayama-u.ac.jp; mkanzaki@misasa.okayama-u.ac.jp.

10.1021/jp992108a CCC: $18.00
Published on Web 11/16/1999

Toplis et al.[2] and Stebbins and Xu[3] have suggested that tricluster oxygen (oxygen shared by three SiO_4 or AlO_4 tetrahedra), first proposed by Lacy,[4] might be a strong candidate for such sites. Stebbins and Xu[3] have proposed that a peak in the ^{17}O 3Q MAS NMR spectrum of the anorthite glass may be a result of such tricluster oxygen. However, their assignment is uncertain because the ^{17}O NMR characteristics of tricluster oxygens are completely unknown.

Another controversial issue is whether Al−O−Al linkage is present to any significant amount in aluminosilicate glasses and melts with Si/Al ≥ 1. This issue is related to the order/disorder of the Si/Al distribution. When the Al/Si distribution is completely ordered, the proportion of Si−O−Si, Si−O−Al, and Al−O−Al BOs are governed by the stoichiometry of the system; Al−O−Al BO appears only when the bulk Si/Al < 1. Whereas when there is disorder in the Si/Al distribution, all three types of BOs in principle can occur. However, the Al−O−Al linkage is generally considered to be energetically unfavorable, accordingly to the Lowenstein's Al avoidance rule.[5] Recent ^{17}O 3Q MAS NMR studies of albite ($NaAlSi_3O_8$, Si/Al = 3)[6] and anorthite (Si/Al = 1)[3] glasses have failed to identify any Al−O−Al linkage in the glass structure. However, as pointed out more recently by Stebbins et al.[7] and also discussed subsequently in the present paper, a peak of the Al−O−Al linkage may actually be present in the ^{17}O 3Q MAS NMR spectrum of the anorthite glass described by Stebbins and Xu.[3] Stebbins et al.[7] have reported ^{17}O 3Q MAS NMR spectra for a sodium aluminosilicate glass with Si/Al = 0.7 and a calcium aluminosilicate glass with Si/Al = 0.5, both of which show two well-resolved peaks that are attributable to Al−O−Al and Si−O−Al BO, respectively. Aluminosilicates with Si/Al < 1, like those described by Stebbins et al.,[7] are expected to contain the Al−O−Al linkage even in the absence of Si/Al disorder and thus represent good reference materials for experimental NMR characterization of such linkages.

As the work of Dirken et al.[6] and Stebbins and Xu[3] have demonstrated, ^{17}O NMR is a promising technique that might put an end to the disputes about the structure of aluminosilicate glasses and melts, such as whether NBO, Al−O−Al BO, or tricluster oxygens are present. These studies also brought up the need to have a better understanding of the NMR characteristics of different oxygen sites, particularly those of the postulated tricluster oxygens. There are two ways to unveil the NMR characteristics of different cation or anion sites. One is to collect NMR spectra for model crystalline phases with known structure, and another is theoretical calculation. Thanks to the development of new NMR techniques for half-integer quadrupolar nuclei, such as the dynamic angle spinning (DAS), double rotation (DOR), and multiple quantum (MQ, including 3Q and 5Q for spin-5/2 nuclei like ^{17}O) MAS NMR methods, there are now increasing, though still limited, experimental ^{17}O NMR data published for the three types of BOs in crystalline materials with known structures.[7−11] Among the various types of triclusters, the $O(Al_3)$ tricluster is the only one that has been identified in a small number of crystalline phases, such as the calcium aluminate $CaAl_4O_7$ phase,[12] although no experimental ^{17}O NMR data have been published for these phases so far and such data should definitely be acquired. The other postulated triclusters (that involve one or more Si) have not been found in any crystalline materials. In this case, theoretical calculation is the only means to reveal their NMR characteristics. Even for structural units, such as the various types of BOs, that can be studied by the experimental NMR approach, there is still a need for a complementary theoretical study, because the latter approach has the advantage of being able to isolate contributions from various structural factors and thus can provide insight into the experimentally observed trends.

The ab initio molecular orbital (MO) calculation method is gaining increasing popularity in predicting geometry and NMR and other spectroscopic properties with the rapid increase in computer power. The early studies on ab initio calculations of the NMR properties of silicates and aluminosilicates, including ^{17}O NMR properties of Si−O−Si, Si−O−Al, and Al−O−Al BOs and $O(Si_3)$ tricluster oxygen, were mostly done by Tossell and co-workers.[13−16] These pioneering studies have demonstrated the power of ab initio calculations in predicting NMR characteristics of local structures. In particular, their results for the ^{17}O quadrupolar coupling parameters, published at a time when experimental ^{17}O data for model crystalline phases were scarce, have often been used for interpreting experimental data of silicate and aluminosilicate glasses.[3,6,17] Accurate calculation of NMR chemical shift was difficult because such calculations require larger basis sets for reliable results; the limited computer power at the time had restricted such studies to small basis sets and/or clusters of restricted structural parameters (e.g., restricted symmetry or bond lengths, or replacing Si−O bond by Si−H bond). The rapid increase in computer power has made it possible now to perform calculations routinely with sufficiently large basis sets at a satisfactorily high level of theory. We have shown in a previous paper[18] that the ^{29}Si and ^{17}O isotropic chemical shifts (δ_i^{Si} and δ_i^{O}) and ^{17}O quadrupolar coupling constant (QCC) calculated at the HF/6-311+G(2df,p) level of theory for Si−O−Si BOs in silicate clusters optimized at HF/6-31G(d) agree well with experimental data for such units in crystalline silicates. Recently, similar calculations, mostly on ^{29}Si and ^{27}Al NMR properties, have also been published for silicate and aluminosilicate clusters of various polymerizations and sizes.[19−21] In this paper, we extend our study to aluminosilicate systems in an attempt to gain insight into the ^{17}O NMR characteristics of different types of BOs (Si−O−Si, Si−O−Al, and Al−O−Al) and tricluster oxygens ($O(Al_3)$, $O(SiAl_2)$, $O(SiAl_2)$, and $O(Si_3)$) that are possibly present in the structure of aluminosilicate glasses and melts. We also report ^{29}Si and ^{27}Al NMR results for these clusters where appropriate. To the best of our knowledge, ab initio calculations have not been conducted, up to now, for the NMR properties of triclusters other than $O(Si_3)$.[15] Similar to our earlier paper[18] on silicate clusters, we have analyzed systematically the effect of other structural factors, such as the T−O−T bond angle (where T stands for a tetrahedrally coordinated cation, such as Si and Al) and the interaction of charge-balancing cations (e.g., Ca^{2+}), because these factors are expected to cause variations in the NMR parameters within each type of structural unit. We have also investigated how the different basis sets and calculation methods affect the resultant NMR parameters.

Calculation Methods

The approach we have taken is to construct small silicate, aluminosilicate, and aluminate clusters that contain the structural units of interest. Considering cluster model for Si−O−Si bridging oxygen in silica (which consists of three-dimensional network of corner-sharing SiO_4 tetrahedra) as an example, there are two ways of terminating the cluster. One is to terminate the cluster at Si and to saturate the dangling bonds by attaching a monovalent atom, commonly H, to Si forming Si−H bonds. This results in a minimal Si_2OH_6 cluster (H-terminated cluster). Another way is to terminate the cluster at O and to saturate the dangling bonds by attaching H to O forming Si−OH bonds.

TABLE 1: Calculated ^{17}O NMR Parameters[a]

cluster	T−O−T angle (deg)	^{17}O QCC[b] (MHz)	EFG η	δ_i^{O}[b](ppm)
		Si−O−Si BO		
$Si_6O_6(OH)_{12}$ 6−ring(C_6)	141.63	(5.30)	(0.12)	(42.75)
$Si_6O_6(OH)_{12}$ 6−ring(D_6)	172.09	(5.80)	(0.17)	(34.31)
$Si_2O(OH)_6$ dimer (C_2)	134.90[c]	5.12 (5.10)	0.40 (0.41)	42.90 (43.09)
$Si_2Al_2O_4(OH)_8^{2-}$ 4-ring (paired Si, Al)	141.87	5.06	0.16	55.20
$Ca(Si_2O(OH)_6)(Al_2O(OH)_6)$ 2-dimer	138.82	5.23	0.22	45.76
		Si−O−Al BO		
$SiAlO(OH)_6^-$ dimer	120	3.33	0.63	43.50
	130	3.50	0.36	39.36
	135.77[c]	3.63	0.16	36.70
	140	3.74	0.10	35.73
	150	3.91	0.19	34.79
	160	3.96	0.18	34.05
	170	3.98	0.14	33.80
	180	3.98	0.11	33.80
$Si_2Al_2O_4(OH)_8^{2-}$ 4-ring (C_2) (alternating Si, Al)	141.62	3.77	0.24	39.88
	132.37	3.63	0.37	39.55
$Si_2Al_2O_4(OH)_8^{2-}$ 4-ring (paired Si, Al)	132.30	3.52	0.28	42.04
	132.84	3.63	0.22	39.75
$Ca(SiAlO(OH)_6)_2$ 2-dimer	133.99	3.43	0.25	46.14
	134.46	3.42	0.25	47.76
		Al−O−Al BO		
$Al_2O(OH)_6^{2-}$ dimer (C_2)	115	1.55	0.62	24.40
	120	1.44	0.99	23.61
	130	1.71	0.50	22.15
	135	1.82	0.34	21.40
	140	1.93	0.22	20.56
	150	2.12	0.04	19.05
	160	2.27	0.07	18.03
	170.66[c]	2.37	0.15	17.59
	180	2.40	0.19	17.54
$Si_2Al_2O_4(OH)_8$ 4-ring (paired Si, Al)	137.68	2.06	0.19	17.12
$Al_4O_4(OH)_8^{4-}$ 4-ring (C_4)	151.83	2.32	0.03	16.51
$Ca(Al_2O(OH)_6)_2^{2-}$ 2-dimer	159.44	1.96	0.06	37.34
$Ca(Si_2O(OH)_6)(Al_2O(OH)_6)$ 2-dimer	133.41	1.82	0.35	56.65
		Tricluster Oxygens		
$Al_3O(OH)_9^{2-}$ tricluster (C_3)	118.39	3.32	0.00	40.29
$O(Al_3)$ tricluster in 3-ring		3.03	0.16	37.73
$SiAl^{IV}Al^{V}O(OH)_9^-$ tricluster		3.21	0.98	59.25
$SiAl^{IV}{}_2O(OH)_8$ tricluster		3.67	0.68	47.48
$O(SiAl_2)$ tricluster in 3-ring		4.08	0.61	47.78
$Si_2AlO(OH)_9$ tricluster		5.22	0.54	65.38
$O(Si_2Al)$ tricluster in 3-ring		5.00	0.70	56.49
$Si_3O(OH)_9^+$ tricluster (C_3)	119.37	6.35	0.00	76.15
$O(Si_3)$ tricluster in 3-ring		6.23	0.04	72.89

[a] All NMR parameters calculated at HF/6-311+G(2df,p) (CSGT method). Values shown in bracket are calculated on HF/6-31G(d) geometries; all the others are on HF/6-31+G(d) geometries. [b] Calculation method: QCC(cluster) = (QCC(H_2O)eq_{zz}(cluster))/eq_{zz}(H_2O), where QCC(H_2O) = 10.175 MHz,[29] eq_{zz}(H_2O) = 1.7783 au for HF/6-31+G(d) geometry and 1.7850 au for HF/6-31G(d) geometry. δ_i^O (cluster) = σ_i^O (TMS) − σ_i^O (cluster), where σ_i^O (TMS) = 318.86 ppm for HF/6-31+G(d) geometry, 318.77 ppm for HF/6-31G(d) geometry. [c] Optimum angle at HF/6-31+G(d).

This leads to a somewhat larger $Si_2O(OH)_6$ cluster (OH-terminated cluster). It is of course also possible to make the cut at more distant Si or O atoms to form even larger clusters. Particularly in early studies when computer power was limited, the first approach was often adopted.[13−16,20] It is clear that this approach does not reproduce the correct first nearest neighbor for Si in SiO_4 tetrahedra and thus does not yield correct δ_i^{Si}. We would like to point out that it does not give correct δ_i^O, or even correct relative order of δ_i^O for BOs and tricluster oxygens either. As an example, we have compared the ^{17}O NMR properties (CSGT method for the shielding calculation) calculated at HF/6-311+G(2df,p) on HF/6-31+G(d) geometries for Al−O−Al BO in $Al_2OH_6^{2-}$ dimer (C_2 symmetry with optimum ∠Al−O−Al = 180.00°), Si−O−Si BO in Si_2OH_6 dimer (C_2 with optimum ∠Si−O−Si = 179.97°), and O(Si_3) tricluster oxygen in $Si_3OH_9^+$ tricluster (C_3 with planar O(Si_3) arrangement) with those of the corresponding sites in OH-terminated clusters of similar T−O−T angle ($Al_2O(OH)_6^{2-}$ dimer, $Si_2O(OH)_6$ dimer and $Si_3O(OH)_9^+$ tricluster). The calculated ^{17}O QCC for the H-terminated clusters (2.94 MHz for Al−O−Al BO in the $Al_2OH_6^{2-}$ dimer, 6.12 MHz for Si−O−Si BO in the Si_2OH_6 dimer and 6.33 MHz for O(Si_3) tricluster oxygen in the $Si_3OH_9^+$ cluster) are not too different from those of the corresponding OH-terminated clusters (2.40 MHz, 5.76 MHz,[18] and 6.35 MHz, respectively; also, see Table 1). On the other hand, the calculated δ_i^O for the H-terminated clusters and OH-terminated clusters do not agree even in the relative order: it decreases from Al−O−Al BO (3.47 ppm), to Si−O−Si BO (−25.73 ppm), to O(Si_3) tricluster oxygen (−31.34 ppm) for the H-terminated clusters, but increases from Al−O−Al BO (17.54 ppm), to Si−O−Si BO (35.56 ppm[18]), to O(Si_3) tricluster oxygen (76.15 ppm) for the OH-terminated clusters (also, see Table 1). Thus, to produce reliable δ_i^O for BOs and tricluster oxygens in aluminosilicates, it is important that the second nearest neighbor is appropriately represented (O instead of H) in the constructed clusters. We would like to note that, although

TABLE 2: Calculated ^{29}Si and ^{27}Al NMR Isotropic Chemical Shifts[a]

cluster	T−O−T angle (deg)	δ_i^{Si}[b] (ppm)	δ_i^{Al}[b] (ppm)
	Si or Al in Q^1 sites		
$Si_2O(OH)_6$ dimer (C_2)	134.90	−79.41(−78.08)	
$SiAlO(OH)_6^-$ dimer	120	−69.33	86.03
	130	−71.53	83.92
	135.77[c]	−73.00	82.60
	140	−74.02	81.77
	150	−76.06	80.41
	160	−77.61	79.97
	170	−78.67	79.84
	180	−79.06	79.77
$Al_2O(OH)_6^{2-}$ dimer (C_2)	115		89.75
	120		88.73
	130		86.98
	135		86.22
	140		85.49
	150		84.21
	160		83.23
	170.66[c]		82.61
	180		82.42
$Ca(SiAlO(OH)_6)_2$ 2-dimer	133.99	−74.63	79.00
	134.46	−75.06	79.14
$Ca(Al_2O(OH)_6)_2^{2-}$ 2-dimer	159.44		82.48
$Ca(Si_2O(OH)_6)(Al_2O(OH)_6)$ 2-dimer: Al−O−Al	133.41		85.15, 81.72
Si−O−Si	138.82	−81.04, −80.57	
	Si or Al in Q^2 Sites		
$Si_6O_6(OH)_{12}$ 6-ring (C_6)	141.63	(−88.56)	
$Si_6O_6(OH)_{12}$ 6-ring (D_6)	172.09	(−97.25)	
$Si_2Al_2O_4(OH)_8$ 4-ring (C_2) (alternating Si, Al)	136.99 (mean value)	−77.37	77.95
$Si_2Al_2O_4(OH)_8$ 4-ring (paired Si, Al)		−79.82, −79.64	80.80, 80.63
$Al_4O_4(OH)_8^{4-}$ 4-ring (C_4)	151.83		76.68
	Si or Al within triclusters (Q^1, Q^2)		
$Al_3O(OH)_9^{2-}$ tricluster (C_3)	118.39		87.81
$O(Al_3)$ tricluster in 3-ring			87.28, 82.25,[d] 81.89[d]
$SiAl^{IV}Al^{V}O(OH)_9^-$ tricluster		−71.00	84.87 (Al^{IV}), 54.96 (Al^{V})
$SiAl^{IV}{}_2O(OH)_8$ tricluster		−76.17	77.78, 78.23
$O(SiAl_2)$ tricluster in 3-ring		−69.68	80.79,[d] 81.76[d]
$Si_2AlO(OH)_9$ tricluster		−73.39, −76.26	84.78
$O(Si_2Al)$ tricluster in 3-ring		−80.56,[d] −81.96[d]	84.03
$Si_3O(OH)_9^+$ tricluster (C_3)	119.37	−77.03	
$O(Si_3)$ tricluster in 3-ring		−77.31, −84.40,[d] −85.97[d]	

[a] Geometries and NMR calculation method same as Table 1. [b] Calculation method: δ_i^{Si} (cluster) = σ_i^{Si} (TMS) − σ_i^{Si} (cluster), δ_i^{Al} (cluster) = σ_i^{Al} ($Al^{3+}(H_2O)_6$) − σ_i^{Al} (cluster), where σ_i^{Si} (TMS) = 385.53 ppm and σ_i^{Al} ($Al^{3+}(H_2O)_6$) = 611.34 ppm for HF/6-31+G(d) geometry; σ_i^{Si} (TMS) = 385.52 ppm for HF/6-31G(d) geometry. [c] Optimum angle at HF/6-31+G(d). [d] Tricluster Al, Si within 3-ring (Q^2).

our result for the ^{17}O QCC (6.33 MHz) of the $O(Si_3)$ tricluster oxygen in the $Si_3OH_9^+$ cluster is close to that of an earlier study of Tossell[15] (6.09 MHz) for a similar cluster with C_{3v} symmetry, the δ_i^O does not agree with the latter study which showed that the $O(Si_3)$ tricluster oxygen has a δ_i^O about 200 ppm larger than that of Si−O−Si BO in Si_2OH_6 dimer. This discrepancy may be due to the fact that the latter study employed smaller basis sets for geometry optimization and NMR shielding calculations and also used the conventional common gauge origin coupled Hartree−Fock theory, which is known to have the problem of showing dependence of NMR shielding on the choice of gauge origin for the vector potential of the magnetic field. In a more recent study, Tossell[22] has also reported that second nearest neighbor has a large effect on the N NMR shielding of $N(Si_3)$ sites in silicon nitride clusters. This may be a general observation for NMR shieldings (chemical shifts) of anions. In the present study, we have adopted the second approach in terminating all the clusters by OH, instead of H. We have performed all the calculations using the Gaussian 94 or Gaussian 98 program.[23]

In the first part of this study, similar to our earlier work[18] on silicate clusters, we first carried out cluster geometry optimization using the Hartree−Fock (HF) method with polarized split-valence 6-31G(d) (for silicate clusters) or 6-31+G(d) basis set (for aluminosilicate and aluminate clusters). We have augmented the 6-31G(d) basis set (also adopted in our earlier study[18] of silicate clusters) with diffuse s, p functions on Si, Al, Ca, and O atoms for aluminosilicate and aluminate clusters because most of these clusters have negative charges. The optimized geometries for all the clusters calculated are true energy minima at the HF/6-31G(d) or HF/6-31+G(d) level because there are no imaginary frequencies. For the neutral $Si_2O(OH)_6$ dimer, the addition of diffuse s, p functions to Si and O atoms results in a minimum energy structure with a Si−O−Si angle of 134.90°, about 3° larger than the angle (131.72°) optimized without the diffuse function (6-31G(d) basis set). The calculated ^{17}O NMR parameters for the optimized HF/6-31+G(d) geometry of the $Si_2O(OH)_6$ dimer are close to those of the 6-31G(d) geometry with identical (fixed) Si−O−Si angle (see Table 1). Thus, the ^{17}O NMR results for neutral silicate clusters of geometries optimized with either basis set are probably directly comparable. The calculated δ_i^{Si} for the optimized HF/6-31+G(d) geometry of the $Si_2O(OH)_6$ dimer is 1.3 ppm smaller (more negative) than that of the 6-31G(d) geometry with identical (fixed) Si−O−Si angle (see Table 2). We have calculated the magnetic shielding and electric field gradient (EFG) tensors using the HF method with the triple split valence 6-311+G(2df,p) basis set. We have adopted the continuous set of gauge transformations (CSGT)

method[24] for the magnetic shielding tensor calculations, to compare directly with our earlier calculations for silicate clusters. We have used the 6-31+G(d) and 6-311+G(2df,p) basis sets implemented in the Gaussian 94 or 98 program for all atoms except Ca. For the 6-31+G(d) basis set of Ca, we have augmented the 6-31G(d) basis set of Rassolov et al.[25] with diffuse s, p functions (exponent, 0.0071). For the 6-311+G-(2df,p) basis set of Ca, we have used the one reported by Blaudeau et al.[26]

The ^{29}Si, ^{27}Al, and ^{17}O isotropic chemical shifts (δ_i^{Si}, δ_i^{Al}, and δ_i^{O}) (in ppm) are calculated relative to the respective reference using the following equation:

$$\delta_i^{\text{Si, Al, or O}}\,(\text{cluster}) = \sigma_i^{\text{Si, Al, or O}}\,(\text{reference}) - \sigma_i^{\text{Si, Al, or O}}\,(\text{cluster}) \tag{1}$$

where σ_i is the isotropic magnetic shielding (in ppm) from the MO calculations. The reference clusters are tetramethylsilane (TMS, $Si(CH_3)_4$) cluster (T_d symmetry) for ^{29}Si, $Al^{3+}(H_2O)_6$ (C_1) for ^{27}Al, and H_2O (C_{2v}) for ^{17}O. The TMS cluster with T_d symmetry results in the same NMR parameters as the TMS cluster with C_3 symmetry (adopted in our earlier study[18]). We have shown previously[18,27,28] that the calculated δ_i^{Si} and δ_i^{O} for silicate clusters of various polymerizations and δ_i^{Al} for isolated aluminate clusters at the level of theory described here are in good agreement with the respective experimental NMR data for similar local structures in crystalline and amorphous silicates or aluminosilicates. We have also pointed out earlier[18] that the δ_i^{O} values for these small clusters are at best representative of those of gas-phase molecules and the medium effect on δ_i^{O} for silicates seems to be significant. Thus, the agreement in the absolute δ_i^{O} values of the small clusters with experimental data of condensed silicates may be accidental. Nevertheless, the relative differences in δ_i^{O} among the silicate clusters are probably directly applicable to condensed silicates.

The ^{17}O QCC and EFG asymmetry parameter (η) are calculated using the following equations:

$$\text{QCC} = e^2 q_{zz} Q/h$$

$$\eta = (eq_{xx} - eq_{yy})/eq_{zz}$$

where eQ is the nuclear quadrupole moment of the nucleus of interest; eq_{xx}, eq_{yy}, and eq_{zz} are the components of the EFG tensor at the nucleus in the principal axis system, with $|eq_{zz}| \geq |eq_{yy}| \geq |eq_{xx}|$. Similar to our previous study,[18] we have estimated the nuclear quadrupole moment eQ for ^{17}O using the experimental ^{17}O QCC value for the H_2O molecule (10.175 ± 0.067 MHz)[29] and the ^{17}O EFG value for the same molecule calculated at the same level of theory (both for geometry optimization and for EFG) as for the aluminosilicate clusters. The advantage of treating the nuclear eQ as an adjustable parameter is that the resultant QCC is insensitive to the basis sets and method used for the geometry optimization or the EFG calculation. The ^{17}O QCC values calculated at the HF/6-311+G(2df,p) level for silicate clusters with HF/6-31G(d) geometries quantitatively agree (mostly within ± 0.1 MHz) with experimental NMR data for crystalline SiO_2[18] (also see subsequent discussion).

In the second part of the study, we have investigated whether the employment of different basis sets and theories (HF vs density functional theory (DFT)) for geometry optimization and for NMR calculations affects the conclusions from the first part of the study. The DFT method is a promising alternative to the traditional correlation methods, such as MP2 (Møller−Plesset second-order perturbation theory). It has been shown to give good results for geometry and vibrational frequencies at a cost on the same order as HF and substantially less than the conventional correlation methods.[30] Cheeseman et al.[31] have compared the performance of HF, DFT, and MP2 methods for NMR chemical shift calculations on a number of small molecules (non-silicates). The result seems to be dependent on the type of the nucleus and the chemical nature of the cluster. There is thus a need to perform a similar test for aluminosilicates. We have adopted the Becke's three-parameter hybrid functional using the correlation functional of Lee, Yang, and Parr (B3LYP)[23] implemented in the Gaussian 94/98 programs for the DFT method. We have performed the cluster geometry optimization and NMR shielding and EFG tensor calculations at both the HF/6-311+G(2df,p) and the B3LYP/6-311+G(2df,p) levels. We have also compared the NMR chemical shifts calculated using the CSGT method with those using the gauge-independent atomic orbital (GIAO) method[31] implemented in the Gaussian 98 program.

Results and Discussion

1. Geometries. *1.1. Models for Si-O-Si BO.* The $Si_2O(OH)_6$ dimer is the simplest OH-terminated cluster to model Si−O−Si BO in silicate glasses and crystals. The optimum geometry has C_2 symmetry with a Si−O−Si angle of 131.72° and Si−O_{br} (O_{br}, BO) bond length of 1.623 Å at the HF/6-31G(d) level.[18] The two parameters become 134.90° and 1.621 Å at the HF/6-31+G(d) level, 140.15° and 1.605 Å at the HF/6-311+G-(2df,p) level, and 132.21° and 1.630 Å at the B3LYP/6-311+G(2df,p) level. In our previous paper,[18] we also calculated several larger silicate clusters containing small silicate rings, including planar (D_3) and puckered (C_1) three-membered rings ($Si_3O_3(OH)_6$), puckered four-membered rings ($Si_4O_4(OH)_8$) (C_4), and double four-membered rings (octamer, $Si_8O_{12}(OH)_8$) (D_4). In this study, we further calculated larger (six-membered) planar and puckered rings ($Si_6O_6(OH)_{12}$) with D_6 and C_6 symmetry, respectively, to test whether the δ_i^{O} of Si−O−Si BO is sensitive to ring size as suggested by Grandinetti et al.[8] The optimum Si−O−Si angle for the $Si_6O_6(OH)_{12}$ six-membered puckered ring (C_6) is 141.63°; that for the planar ring (D_6) is 172.09° at the HF/6-31G(d) level.

1.2. Models for Si−O−Al BO. The $SiAlO(OH)_6^-$ dimer is the simplest OH-terminated cluster to model Si−O−Al BO in aluminosilicate glasses. The optimum Si−O−Al angle at the HF/6-31+G(d) level is 135.77°. This angle varies only slightly at higher levels (137.34° at HF/6-311+G(2df,p), 133.45° at B3LYP/6-311+G(2df,p)). The optimum Si−O_{br} and Al−O_{br} bond lengths are 1.591 and 1.771 Å, respectively, at HF/6-31+G(d), 1.576 and 1.755 Å at HF/6-311+G(2df,p), and 1.602 and 1.776 Å at B3LYP/6-311+G(2df,p). We have performed calculations for $SiAlO(OH)_6^-$ dimers optimized without constraints and with the constraint of fixed Si−O−Al angle from 120° to 180° to investigate the Si−O−Al angle dependence of the NMR parameters. We have also performed the calculation for two $Si_2Al_2O_4(OH)_8^{2-}$ four-membered ring clusters at the HF/6-31+G(d) level: one with alternating Al and Si distribution (C_2 symmetry) and another with paired Al and Si distribution. The energy at HF/6-311+G(2df,p) for the former (−1966.08557 hartree) is lower than that of the latter (−1966.06674 hartree) by 0.01883 hartree (49.4 kJ/mol), consistent with the result of Tossell and Sághi-Szabó[20] for similar clusters. These calculations provide the theoretical basis for the Lowenstein's Al avoidance rule. The $Si_2Al_2O_4(OH)_8^{2-}$ four-membered ring with alternating Al and Si distribution is puckered with Si−O−Al angles of 132.37° and 141.62°. The cluster with paired Al and Si distri-

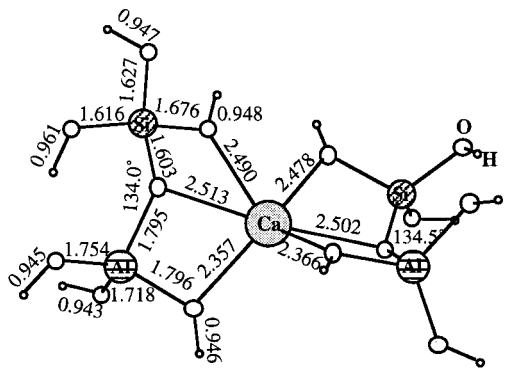

$Ca(SiAlO(OH)_6)_2$ double-dimer

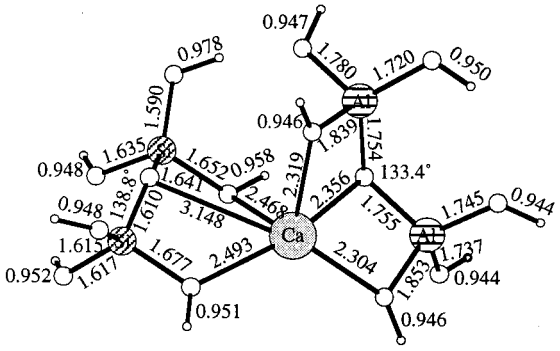

$Ca(Si_2O(OH)_6)(Al_2O(OH)_6)$ double-dimer

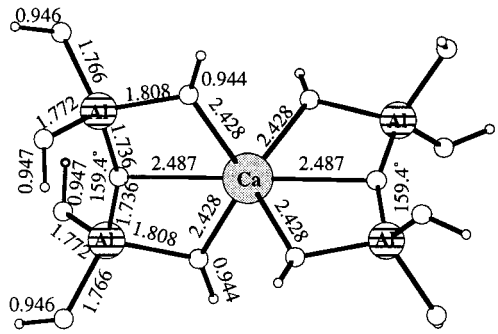

$Ca(Al_2O(OH)_6)_2^{2-}$ double-dimer

Figure 1. Optimized geometries at HF/6-31+G(d) for Ca^{2+}-linked double dimers. Numbers shown are values of the bond length (Å) and bond angle (deg).

bution contains two Si−O−Al linkages (132.30° and 132.84°), one Si−O−Si linkage (141.87°), and one Al−O−Al linkage (137.68°).

In aluminosilicate glasses or crystalline phases, the Si−O−Al BOs are often also bonded to one or more charge-balancing cations, such as Ca^{2+}. To model such a situation, we have constructed the $Ca(SiAlO(OH)_6)_2$ cluster, which consists of two $SiAlO(OH)_6^-$ dimers linked by Ca^{2+} (Figure 1). In this cluster, Ca^{2+} is coordinated to six oxygens, two of which are BOs at distances of 2.50−2.51 Å, and four of which are hydroxyl (OH) oxygens at distances of 2.36−2.49 Å at the HF/6-31+G(d) level. The oxygen coordination number of Ca^{2+} is similar to those in crystalline aluminosilicates, such as $CaAl_2Si_2O_8$ anorthite.[32] Each Si−O−Al BO in the cluster is bonded to one Ca^{2+}. The two Si−O−Al angles are 133.99° and 134.46°, close to the optimum Si−O−Al angle of isolated $SiAlO(OH)_6^-$ dimer. The energy at HF/6-311+G(2df,p) for this cluster (−2795.15974 hartree) is lower by 0.04055 hartree (106.5 kJ/mol) than that of the $Ca(Si_2O(OH)_6)(Al_2O(OH)_6)$ cluster (described below), which consists of a $Al_2O(OH)_6^{2-}$ dimer and a $Si_2O(OH)_6$ dimer linked by Ca^{2+} (−2795.11919 hartree). This result is consistent with the Lowenstein's Al-avoidance rule.

1.3. Models for Al−O−Al BO. The $Al_2O(OH)_6^{2-}$ dimer is the simplest OH-terminated cluster to model Al−O−Al BOs in aluminates and aluminosilicates. The optimum geometry has C_2 symmetry with an Al−O−Al angle of 170.66° at HF/6-31+G(d) level. This angle is larger than those in many crystalline aluminates (e.g., 132° for crystalline $KAl_2O(OH)_6$;[33] 115−132° for crystalline $CaAl_2O_4$[34]), possibly due to the repulsion of the negative charges. The optimum Al−O−Al angle varies only slightly at higher levels (171.32° at HF/6-311+G-(2df,p); 170.22° at B3LYP/6-311+G(2df,p)). The optimum $Al-O_{br}$ bond length is 1.726 Å at HF/6-31+G(d), 1.710 Å at HF/6-311+G(2df,p), and 1.730 Å at B3LYP/6-311+G(2df,p). We have also performed calculations for $Al_2O(OH)_6^{2-}$ dimers optimized with C_2 symmetry and under the constraint of fixed Al−O−Al angle from 115° to 180° at HF/6-31+G(d) level to investigate the Al−O−Al angle dependence of the NMR parameters. In addition, we have studied the more polymerized $Al_4O_4(OH)_8^{4-}$ four-membered ring cluster (C_4 symmetry). The ring is nearly planar with Al−O−Al angles of 151.83° at HF/6-31+G(d).

Similar to the approach to the Si−O−Al BO, we have also constructed two Ca^{2+}-sandwiched double dimer clusters, $Ca(Si_2O(OH)_6)(Al_2O(OH)_6)$ and $Ca(Al_2O(OH)_6)_2^{2-}$, to model the more realistic situation of Al−O−Al BOs charged-balanced by other cations (Figure 1). The $Ca(Si_2O(OH)_6)(Al_2O(OH)_6)$ cluster consists of a $Al_2O(OH)_6^{2-}$ dimer and a $Si_2O(OH)_6$ dimer linked by Ca^{2+}. In this cluster, Ca^{2+} is coordinated to six oxygens, one of which is Al−O−Al BO at a distance of 2.36 Å, another of which is Si−O−Si BO at a longer distance of 3.15 Å, and four of which are hydroxyl oxygens at 2.30−2.49 Å at the HF/6-31+G(d) level. Both the Al−O−Al and the Si−O−Si BOs are bonded to one Ca^{2+}, although the latter is much weaker. The Al−O−Al angle for the $Al_2O(OH)_6^{2-}$ dimer is 133.41° and the Si−O−Si angle for the $Si_2O(OH)_6$ dimer is 138.82°. The $Ca(Al_2O(OH)_6)_2^{2-}$ double dimer cluster consists of two $Al_2O(OH)_6^{2-}$ dimers linked by Ca^{2+}. In this cluster, Ca^{2+} is coordinated to six oxygens, two of which are BOs at a distance of 2.49 Å and four are hydroxyl oxygens at 2.43 Å at HF/6-31+G(d). Each Al−O−Al BO is bonded to one Ca^{2+}. The Al−O−Al angles for the two $Al_2O(OH)_6^{2-}$ dimers are 159.45°.

1.4. Models for $O(Si_{3-x}Al_x)$ Tricluster Oxygens. We have constructed $Si_{3-x}Al_xO(OH)_9^{(x-1)-}$ clusters as models for isolated triclusters (Figure 2). The $Al_3O(OH)_9^{2-}$ tricluster was optimized under the constraint of C_3 symmetry. Each Al is tetrahedrally coordinated to four O atoms. At HF/6-31+G(d), the Al−O−Al angles are 118.39°; thus, the $O(Al_3)$ arrangement is slightly off planarity. The $Al-O_{tri}$ (O_{tri}, tricluster oxygen) bond lengths are 1.830 Å, similar to those of the crystalline $CaAl_4O_7$ phase (1.78−1.80 Å).[12] This bond is longer than the $Al-O_{br}$ bond of the $Al_2O(OH)_6^{2-}$ dimer (1.726 Å), as expected because the tricluster oxygen in the former is more excessively bonded than the BO in the latter. The Al−O lengths for Al−OH bonds (1.75−1.78 Å) are shorter than the $Al-O_{tri}$ length. The $Al-O_{tri}$ bond lengths become 1.819 Å at HF/6-311+G(2df,p) and 1.833 Å at B3LYP/6-311+G(2df,p).

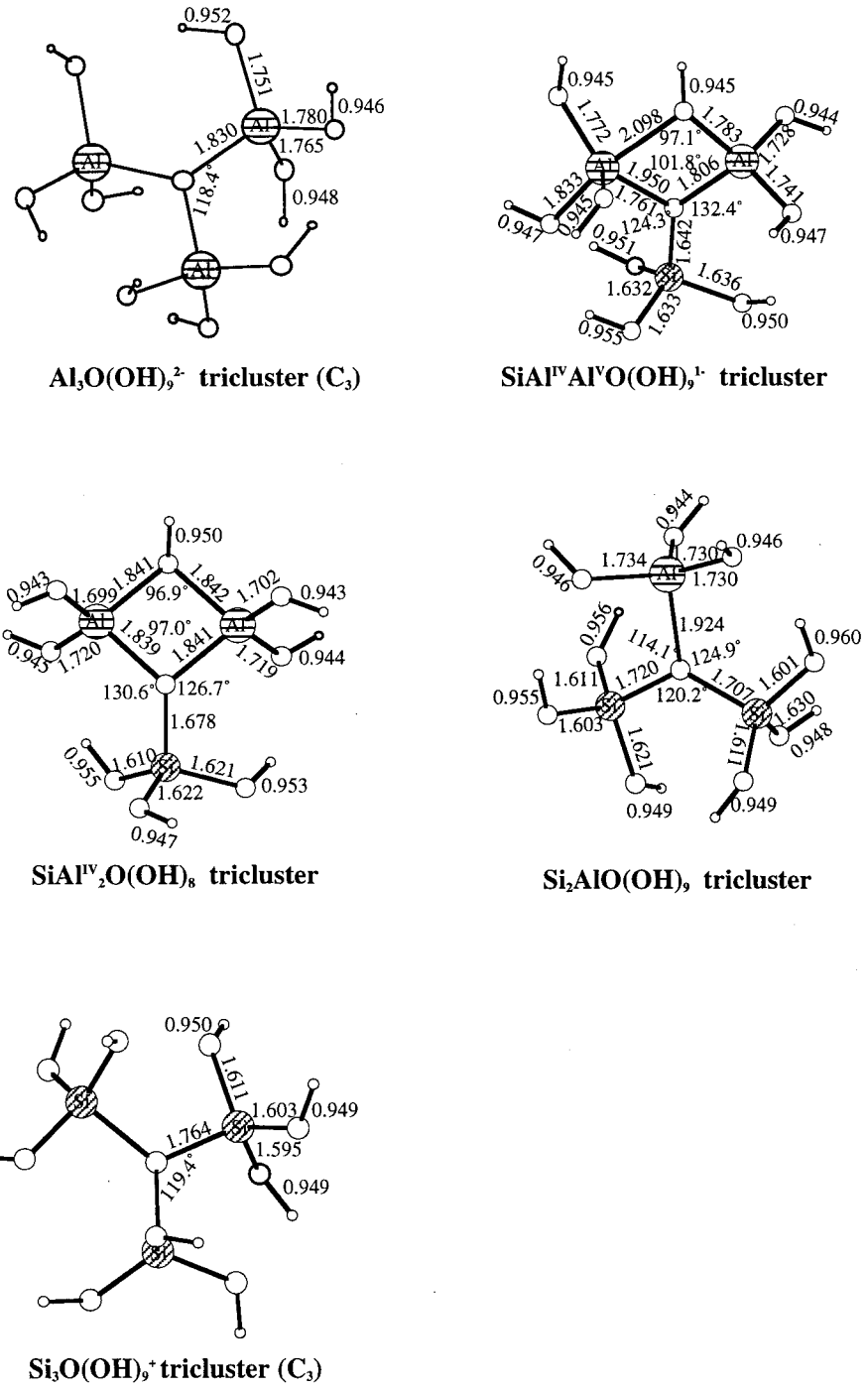

Figure 2. Optimized geometries at HF/6-31+G(d) for isolated $O(Si,Al)_3$ triclusters. Symbols and labels same as Figure 1.

In the optimized geometry for $SiAl_2O(OH)_9^-$ tricluster, one of the Al atoms turned out to be five-coordinated (Al^V), whereas the other Al and the Si atom are tetrahedrally coordinated (Figure 2). The formation of Al^V is due to the local charge imbalance. This should not be taken as evidence against the stability of $O(SiAl^{IV}_2)$ tricluster, but should be considered as an artifact due to the small size of the cluster. As shown below, Al^V does not form once the tricluster is incorporated into a ring structure. At HF/6-31+G(d), the $Si-O_{tri}$ distance is 1.642 Å, only slightly longer than the $Si-O_{br}$ bond length in $Si_2O(OH)_6$ dimer (1.621 Å). The $Al^{IV}-O_{tri}$ distance is 1.806 Å, slightly shorter than that of the $Al_3O(OH)_6^{2-}$ tricluster. The Al^V-O_{tri} distance is 1.950 Å, similar to the those of $Al(OH)_5^{2-}$ cluster (1.85−1.98 Å).[28] The Al^V-O bond (2.098 Å) of the $Al^V-OH-Al^{IV}$ linkage is longer than the other Al^V-OH bonds (1.76−1.83 Å).

One way to avoid the formation of Al^V in isolated $O(SiAl_2)$ tricluster is to simply remove one of the hydroxyls from the $SiAl_2O(OH)_9^-$ cluster. The resultant $SiAl_2O(OH)_8$ tricluster contains two edge-sharing Al (Figure 2). All Si and Al in this cluster are tetrahedrally coordinated. At HF/6-31+G(d), the Al−O−Al angle is 97.01° and the two Si−O−Al angles are 130.63° and 126.74°. The $Si-O_{tri}$ distance is 1.679 Å, and the $Al-O_{tri}$ distances are 1.839 and 1.841 Å.

In the optimized $Si_2AlO(OH)_9$ tricluster, all Si and Al are tetrahedrally coordinated (Figure 2). At HF/6-31+G(d), the Si−O−Si angle is 120.21° and the two Al−O−Al angles are 114.08° and 124.92°. The lengths of the two $Si-O_{tri}$ bonds are

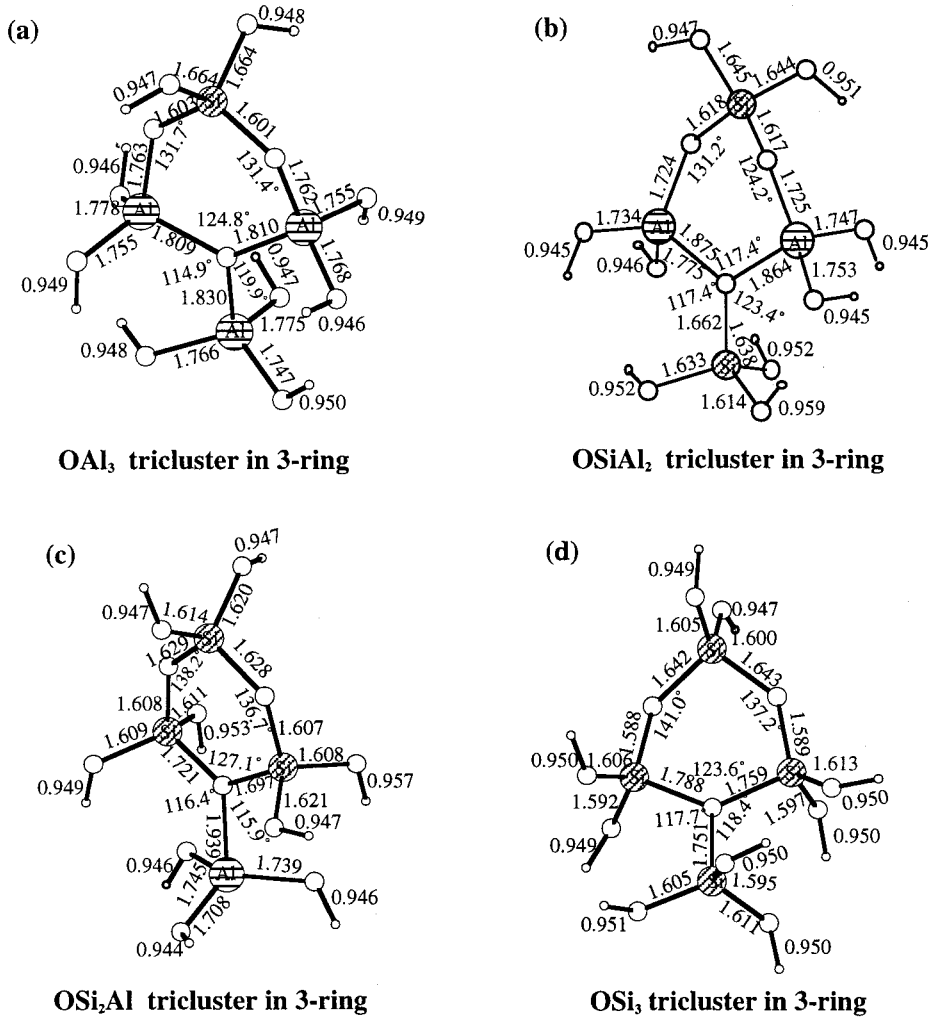

Figure 3. Optimized geometries at HF/6-31+G(d) for O(Si,Al)$_3$ triclusters in a three-membered ring: (a) $SiAl_3O_3(OH)_9^{2-}$; (b) $Si_2Al_2O_3(OH)_9^{-}$; (c) $Si_3AlO_3(OH)_9$; (d) $Si_4O_3(OH)_9^{+}$. Symbols and labels same as Figure 1.

1.707 and 1.720 Å, longer than those in the $SiAl_2O(OH)_8$ tricluster. This is expected because the tricluster oxygen in the former is more excessively bonded than that in the latter. The Al−O_{tri} bond length is 1.924 Å, longer than that in either $Al_3O(OH)_9^{2-}$ tricluster or $SiAl_2O(OH)_8$ tricluster, again as expected.

The $Si_3O(OH)_9^{+}$ tricluster was optimized under the constraint of C_3 symmetry. Each Si is tetrahedrally coordinated to four O atoms (Figure 2). At HF/6-31+G(d), the Si−O−Si angles are 119.37°. The Si−O_{tri} (O_{tri}, tricluster oxygen) bond lengths are 1.764 Å, the longest among the four types of triclusters. From bond strength consideration, this type of tricluster is probably least likely to be present in the aluminosilicate structure.

We have also constructed $Si_{4-x}Al_xO_3(OH)_9^{(x-1)-}$ clusters that represent O($Si_{3-x}Al_x$) triclusters in a three-membered ring (Figure 3), in an attempt to investigate how the degree of polymerization affects the NMR properties of O, Si, and Al within the tricluster. All Al and Si in these clusters are tetrahedrally coordinated. The Al−O_{tri} and Si−O_{tri} bond lengths are similar to those of the isolated triclusters. For the description of the degree of polymerization of tetrahedral cations in aluminosilicates that do not contain triclusters, the Q^n notation is often adopted. In this notation, a SiO_4 or AlO_4 tetrahedron of Q^n speciation (where $n = 0-4$) shares n oxygens with n other SiO_4 or AlO_4 tetrahedra. The tricluster Al/Si within the three-membered ring are described subsequently as Al/Si (Q^2), like the other Al/Si within ring structure, because each shares two oxygens with other Si(Al)O_4 tetrahedra. Similarly, tricluster Al/Si outside the ring are described as Al/Si (Q^1), although the number of Si(Al)O_4 neighbors for tricluster Si/Al (Q^n) are actually $n + 1$.

2. NMR Characteristics at the HF/6-311+G(2df,p) Level with HF/6-31G(d) or 6-31+G(d) Geometry. *2.1. Si−O−Si BO.* Among the three types of BOs, Si−O−Si BOs, particularly those in SiO_2 polymorphs, are ideal for checking the reliability of theoretical calculations, because these BOs are not bonded to any charge-balancing cations and thus can be adequately modeled by small silicate clusters.

As presented in our earlier paper,[18] and also shown in Figure 4, the calculated ^{17}O QCC values for Si−O−Si BOs in silicate clusters agree well (mostly within 0.1 MHz) with the experimental data for SiO_2 polymorphs (cristobalite[35] and coesite[8]). Both the calculation and experimental data suggest that the ^{17}O QCC of Si−O−Si BO depends dominantly on the Si−O−Si angle (Figure 4) and is thus a useful parameter that can be used to decipher Si−O−Si angle distribution information for silicate glasses. The EFG asymmetry parameter, η, for Si−O−Si BO in the $Si_2O(OH)_6$ dimer (C_2 symmetry) decreases with increasing Si−O−Si angle. Data for the other silicate clusters, however, deviate from the trend defined by the dimers (Figure 4), suggesting that η is sensitive to the symmetry of the local structure and thus is not a reliable parameter for predicting Si−O−Si angle in silicates. Vermillion et al.[36] have recently performed similar calculations on $Si_2O(OH)_6$ dimers (at HF/6-31+G(d) for

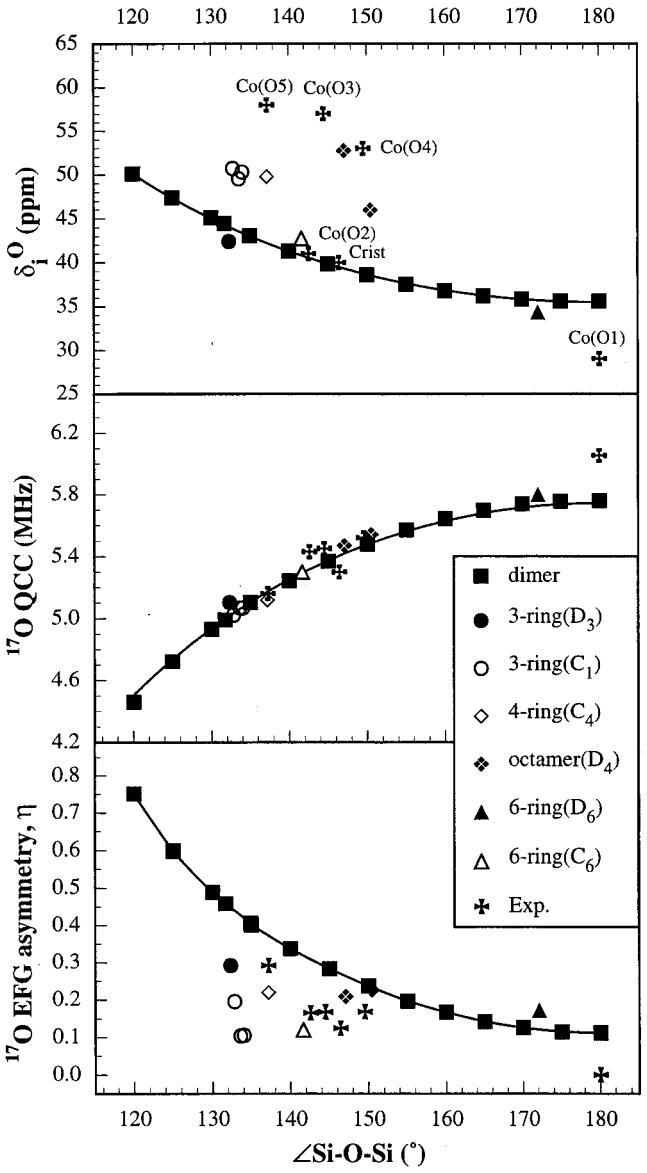

Figure 4. ^{17}O isotropic chemical shift (δ_i^O, upper), QCC (middle) and EFG asymmetry parameter, η (lower), as a function of Si−O−Si angle for Si−O−Si BOs in $Si_2O(OH)_6$ dimer (C_2 symmetry), $Si_3O_3(OH)_6$ planar (D_3) and puckered (C_1) three-membered rings, $Si_4O_4(OH)_8$ puckered four-membered ring (C_4), $Si_8O_{12}(OH)_8$ double puckered four-membered ring (octamer, D_4), as well as $Si_6O_6(OH)_{12}$ planar (D_6) and puckered (C_6) six-membered rings; all calculated at HF/6-311+G(2df,p) (CSGT method) with HF/6-31G(d) geometries. Data for the two six-membered ring clusters are from this study; others are from Xue and Kanzaki.[18] Curves are spline fit to the data for the $Si_2O(OH)_6$ dimer. Also shown are experimental NMR data of SiO_2 polymorphs cristobalite (Crist)[35] and coesite (Co).[8] The O site of cristobalite and O1 and O2 sites of coesite are part of a six- or eight-membered ring structure; the O3, O4, and O5 sites of coesite are part of a four-membered ring structure.

both geometry optimization and EFG calculation) with and without alkali cations (Li, Na) coordinated to the BO. Their calculated ^{17}O QCC and η values for Si−O−Si BO in the $Si_2O(OH)_6$ dimer exhibit similar trend to those shown in Figure 4, although their η values are smaller than ours by about 0.1 but are similar to those of the Si_2OH_6 dimer.[14,15] The discrepancy in the calculated η values of Vermillion et al.[36] and ours is likely due to the different orientations of the Si−O−H bonds in the dimer clusters adopted in the two studies, and is in itself evidence that η is sensitive to the symmetry of local structures. Vermillion et al.[36] have also shown that the ^{17}O QCC of the Si−O−Si BOs are reduced, when coordinated to one or more alkali cations, consistent with experimental observations.

The calculated δ_i^O of the Si−O−Si BOs in silicate clusters also show reasonable agreement with the experimental data for SiO_2 polymorphs (Figure 4). However, as revealed in section 3.3, the absolute values of δ_i^O change considerably when different method for the shielding calculations (GIAO) or different theory (DFT) are used, the agreement is thus accidental. Nevertheless, the relative changes among the silicate and aluminosilicate clusters do not vary as much with the calculation methods and should thus be more reliable. For the simple $Si_2O(OH)_6$ dimer, the δ_i^O of Si−O−Si BO decreases with increasing Si−O−Si angle (Figure 4). The δ_i^O of the Si−O−Si BOs in the other silicate clusters, however, show large variations that cannot be solely accounted for by the Si−O−Si angle (Figure 4). There is a need to understand the structural factors that are responsible for such variations before comparisons are made with different types of BOs or with other types of oxygen sites such as tricluster oxygens. Our previous calculations[18] suggest that the ring puckering affects the δ_i^O: Si−O−Si BOs in puckered three- or four-membered rings give larger δ_i^O than those in the $Si_2O(OH)_6$ dimer or planar rings (that have higher energy than the puckered ones). Grandinetti et al.[8] have noted from experimental ^{17}O NMR data for SiO_2 polymorph coesite that Si−O−Si BOs in small (four-membered) rings give larger δ_i^O than those in larger (six-membered or larger) rings (also see Figure 4). To test whether this is a general conclusion that can be reproduced in calculations, we have also carried out calculations for $Si_6O_6(OH)_{12}$ six-membered rings (both planar and puckered) in this study. The Si−O−Si BOs in both planar (D_6 symmetry) and puckered (C_6) six-membered rings give δ_i^O that are similar to those of the dimer, but lower than those of three- and four-membered puckered rings (Table 1, Figure 4), suggesting that the observation of Grandinetti et al.[8] may be generally applicable. In brief, the present calculation and the available experimental data together suggest that the δ_i^O of Si−O−Si BO in silicates depends on the Si−O−Si angle and the puckering and size of the ring within which the linkage is incorporated; the δ_i^O is larger for Si−O−Si BO with smaller Si−O−Si angle and even larger for Si−O−Si BO in puckered small (three- or four-membered) rings.

One question is whether the ^{17}O NMR results for Si−O−Si BOs in silicate clusters are applicable to aluminosilicates, for which further complication could arise as a result of different Al/Si distributions beyond the second coordination sphere of Si. Among the aluminosilicate clusters we have considered, only two contain Si−O−Si linkages: one is the $Si_2Al_2O_4(OH)_8^{2-}$ four-membered ring with paired Si and Al distribution; another is the Ca^{2+}-sandwiched double-dimer cluster, $Ca(Si_2O(OH)_6)(Al_2O(OH)_6)$. The ^{17}O QCC of the former falls on the trend defined by the silicate clusters, whereas that of the latter is about 0.2 MHz lower (not shown in Figure 4; see Table 1). The discrepancy for the latter could be due to (weak) interaction of the Ca^{2+} cation with the Si−O−Si BO. Thus, it seems likely that the correlation between ^{17}O QCC and Si−O−Si angle shown by silicates might be applicable to aluminosilicates as well, when the Si−O−Si BO is not coordinated to other cations, although more test is clearly needed. The δ_i^O of the Si−O−Si BOs in the $Si_2Al_2O_4(OH)_8^{2-}$ four-membered ring and the $Ca(Si_2O(OH)_6)(Al_2O(OH)_6)$ double dimer are about 4 and 15 ppm, respectively, above the trend shown by the $Si_2O(OH)_6$ dimer (not plotted in Figure 4; see Table 1). The former may be a result of the small (four-membered) ring structure, whereas the

latter may be explained by cation interaction because it is known from experimental observations that interaction of high field strength cations, such as Ca^{2+}, with Si−O−Si BOs tends to cause deshielding (larger δ_i^O) of the oxygen.[37]

The δ_i^{Si} of the puckered and planar $Si_6O_6(OH)_{12}$ six-membered rings are −88.56 and −97.25 ppm, respectively, close to those of Si (Q^2) in $Si_3O_2(OH)_8$ linear trimer of similar Si−O−Si angles.[18]

2.2. Si−O−Al and Al−O−Al BOs. The Si−O−Al BOs in all the calculated clusters (dimer, four-membered ring, and Ca^{2+}-linked double dimer) give ^{17}O QCC in the range of 3.3−4.0 MHz and δ_i^O of 33.8−47.8 ppm, in general agreement with experimental data of zeolites (3.2−4.2 MHz and 25−50 ppm[10,11]). Compared with Si−O−Si BO, the Si−O−Al BOs in general have smaller ^{17}O QCC and overlapping δ_i^O (see Figure 7). For the simple $SiAlO(OH)_6^-$ dimer, the δ_i^O of Si−O−Al BO decreases and the ^{17}O QCC increases with increasing Si−O−Al angle (Figure 5), a trend similar to that for Si−O−Si BO (Figure 4). Xu and Stebbins[10] have noted from ^{17}O two-dimensional DAS NMR data for the zeolite stilbite that the δ_i^O of Si−O−Al BOs increases with increasing ^{17}O QCC. This pattern is opposite to our calculation for the $SiAlO(OH)_6^-$ dimer and thus has to be attributed to structural variations other than the Si−O−Al angle. The EFG asymmetry parameter, η, of the $SiAlO(OH)_6^-$ dimer does not show a monotonic trend with the Si−O−Al angle, apparently due to the lack of symmetry at the oxygen site. Nevertheless, this parameter is ≤ 0.5 for most angles (all angles $>120°$), consistent with experimental observations.[10,11] The ^{17}O QCC of Si−O−Al BOs in the two $Si_2Al_2O_4(OH)_8^{2-}$ four-membered ring clusters with alternating and paired Al and Si distributions are similar to those of the $SiAlO(OH)_6^-$ dimer (Figure 5). The ^{17}O QCC of the Si−O(Ca)-Al BOs in the Ca^{2+}-linked double dimer are smaller by about 0.2 MHz than the Si−O−Al BOs in the $SiAlO(OH)_6^-$ dimer, suggesting that interaction of Ca^{2+} tends to lower the ^{17}O QCC of the BOs. This result is consistent with experimental observations for Si−O−Si BOs.[18] The δ_i^O shows larger variations than the ^{17}O QCC. The Si−O−Al BOs in the four-membered rings give larger δ_i^O than those of the $SiAlO(OH)_6^-$ dimer, similar to the trend for Si−O−Si BOs. The largest δ_i^O are from the Si−O(Ca)−Al BOs in the Ca^{2+}-linked double dimer cluster (Figure 5). This is clearly the effect of interaction of the Ca^{2+} cation, a result consistent with experimental observations that Si−O(Ca)−Al BO in anorthite glass gives larger δ_i^O than Si−O−Al BOs in albite glass or in zeolites.[3] It should be pointed out that, in this simplified cluster, each Si−O−Al BO is bonded to one Ca^{2+}, whereas in actual aluminosilicate crystals or glasses, each BO may be bonded to zero to more than one Ca^{2+}. For example, in the crystalline $CaAl_2Si_2O_8$ anorthite phase, each Si−O−Al BO is bonded to either zero, one, or two Ca^{2+}.[32] Thus, the δ_i^O for the latter case are expected to show a larger range of values (both smaller and larger) than those calculated for the simplified double-dimer cluster.

The Al−O−Al BOs in all the calculated clusters give small ^{17}O QCC of 1.4−2.4 MHz and a range of δ_i^O from 16.5 to 56.7 ppm, in reasonable agreement with the recently published experimental ^{17}O NMR data for Al−O−Al BOs in crystalline $CaAl_2O_4$ (P_Q = 1.5−2.4 MHz, δ_i^O = 39.3−87.2 ppm; where $P_Q = QCC(1 + \eta^2/3)^{1/2}$, which is 0−15% greater than QCC, depending on the value of EFG asymmetry parameter η that is in the range 0−1) and $NaAlO_2$ (P_Q = 1.8 MHz, δ_i^O = 30.9 ppm) phases.[7] As was also shown by previous ab initio calculations of Tossell[16] at lower levels of theory, Al−O−Al BOs are characterized by small ^{17}O QCC. For the Al−O−Al BO in the $Al_2O(OH)_6^{2-}$ dimer, the δ_i^O decreases with increasing Al−O−Al angle (Figure 6, Table 1), similar to the trend for Si−O−Si and Si−O−Al BOs. The ^{17}O QCC increases with increasing Al−O−Al angle above 120°, but increases again at smaller angle, which is associated with a change in the orientation of the EFG tensor at 120°. The EFG asymmetry parameter, η, shows an opposite trend to that of the ^{17}O QCC, with a maximum of 0.99 at 120°(Figure 6, Table 1). It is worthwhile to note that unlike what is often observed for typical Si−O−Si or Si−O−Al BOs,[7] this parameter is large (≥ 0.5) for Al−O−Al BOs with small angles, which are common in many crystalline aluminates (e.g., 115−132° for the $CaAl_2O_4$ phase[34]). Because it is P_Q (=$QCC(1 + \eta^2/3)^{1/2}$), rather than QCC, that is often estimated from DAS or MQ MAS NMR data, a knowledge of the relative magnitude of η is important. For example, at 120° of Al−O−Al angle when η has a large

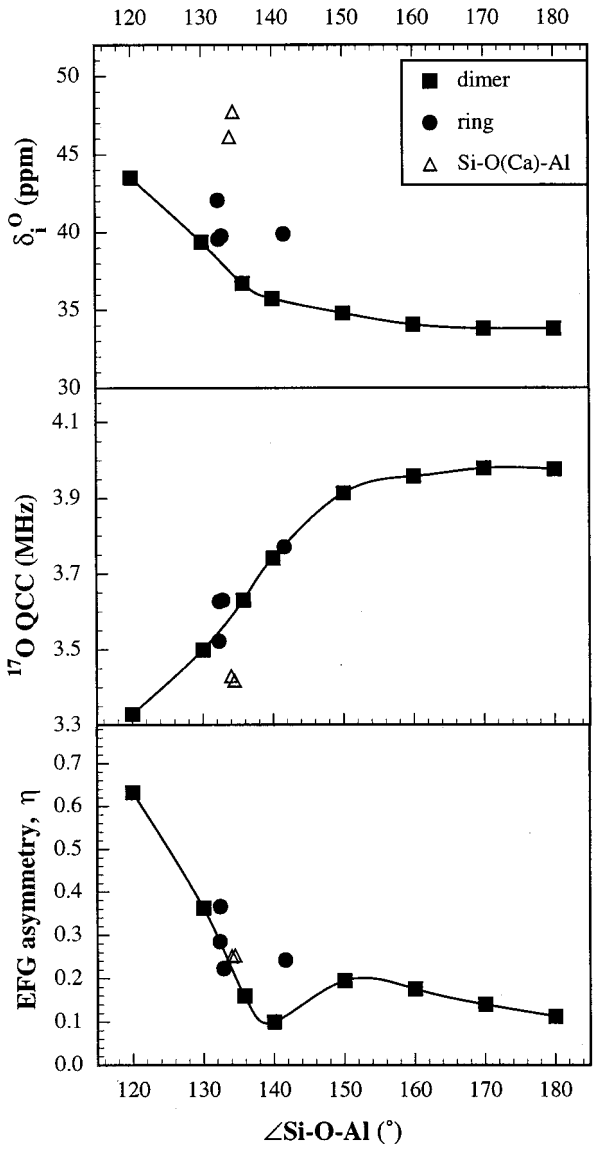

Figure 5. ^{17}O isotropic chemical shift (δ_i^O, upper), QCC (middle) and EFG asymmetry parameter, η (lower), as a function of Si−O−Al angle for Si−O−Al BOs in $SiAlO(OH)_6^-$ dimer, two $Si_2Al_2O_4(OH)_8^{2-}$ four-membered rings, one with alternating Si, Al distribution (C_2) and another with paired Si, Al distribution, and $Ca(SiAlO(OH)_6)_2$ Ca^{2+}-linked double dimer. All calculated at HF/6-311+G(2df,p) (CSGT method) with HF/6-31+G(d) geometries. Curves are spline fit to the data for the $SiAlO(OH)_6^-$ dimer.

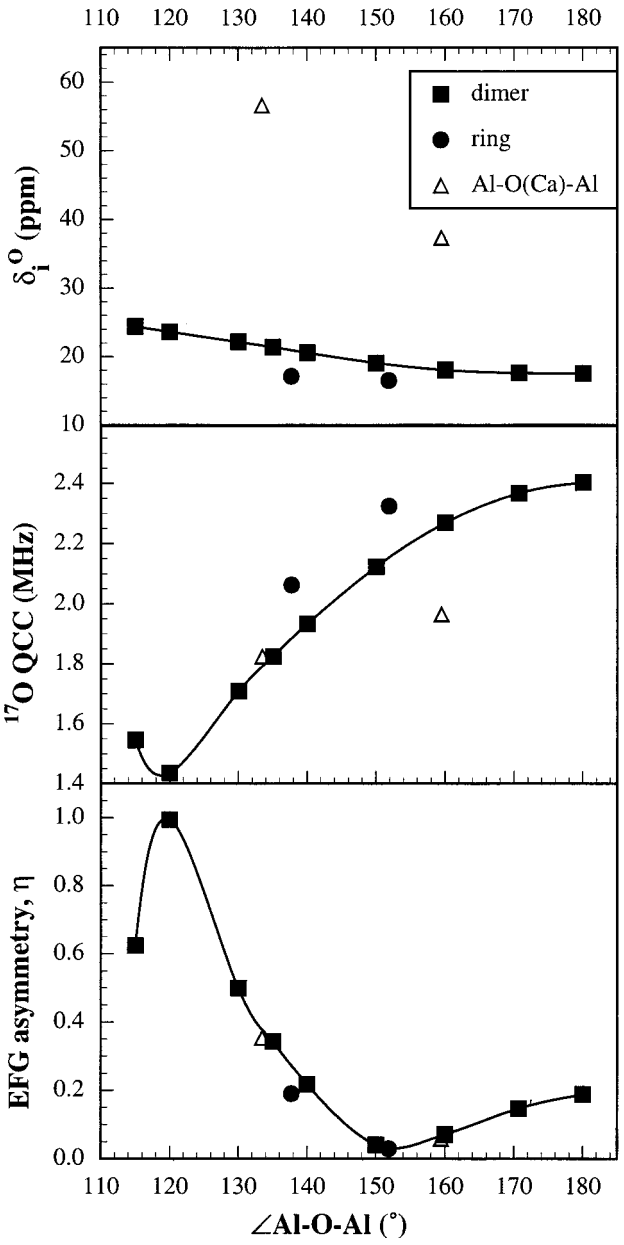

Figure 6. ^{17}O isotropic chemical shift (δ_i^O, upper), QCC (middle) and EFG asymmetry parameter, η (lower), as a function of Al−O−Al angle for Al−O−Al BOs in $Al_2O(OH)_6^{2-}$ dimer, $Al_4O_4(OH)_8^{4-}$ and $Si_2Al_2O_4(OH)_8^{2-}$ (paired Si, Al distribution) four-membered rings, and $Ca(Si_2O(OH)_6)(Al_2O(OH)_6)$ and $Ca(Al_2O(OH)_6)_2^{2-}$ Ca^{2+}-linked double dimer clusters. All calculated at HF/6-311+G(2df,p) (CSGT method) with HF/6-31+G(d) geometries. Curves are spline fit to the data for the $Al_2O(OH)_6^{2-}$ dimer.

value of 0.99, P_Q is 15% greater than QCC. The ^{17}O QCC of Al−O−Al BOs in the $Al_4O_4(OH)_8^{4-}$ and $Si_2Al_2O_4(OH)_8^{2-}$ (paired Al distribution) four-membered rings are both about 1.5 MHz larger than those of the dimers. The ^{17}O QCC of the Al−O(Ca)−Al BOs in the two types of Ca^{2+}-linked double-dimer clusters are either similar or 0.3 MHz smaller than the Al−O−Al BOs in the dimers, again suggesting that interaction of Ca^{2+} has a tendency to lower the ^{17}O QCC of the BOs, though to a varying degree. The δ_i^O of Al−O(Ca)−Al BOs in the two Ca^{2+}-linked double-dimer clusters (37.3 and 56.7 ppm) are significantly larger (by about 20−40 ppm) than Al−O−Al BOs in the simple $Al_2O(OH)_6^{2-}$ dimer, indicating that interaction of Ca^{2+} with Al−O−Al BO tends to increase its δ_i^O, consistent with the experimental data for the crystalline $CaAl_2O_4$ phase.[7]

As was also discussed for the Si−O−Al BO above, each Al−O−Al is charge-balanced by only one Ca^{2+} in these simplified double-dimer clusters, whereas those in actual aluminosilicate and aluminate crystals or glasses may be bonded to zero to more than one Ca^{2+} (e.g., the 12 BO sites in the $CaAl_2O_4$ phase are bonded to either one or two Ca^{2+} [34]); thus, the δ_i^O for the latter case are expected to show a greater range of values than those calculated here for the simple clusters.

The δ_i^{Al} and δ_i^{Si} of the Si/Al (Q^1) in $SiAlO(OH)_6^-$ dimer and the δ_i^{Al} of the Al (Q^1) in $Al_2O(OH)_6^{2-}$ dimer all decrease with increasing T−O−T angle (Table 2 and Figure 7), a trend similar to the δ_i^{Si} of silicate clusters.[18] The δ_i^{Al} and δ_i^{Si} of the Si/Al (Q^2) in the $Al_4O_4(OH)_8^{4-}$ and $Si_2Al_2O_4(OH)_8^{2-}$ (alternating Si, Al distribution) four-membered rings are a few ppm smaller than those of Si/Al (Q^1) in the corresponding dimers with similar T−O−T angle (see Table 2). This trend of increasing cation chemical shift with decreasing degree of polymerization has also been observed for silicate clusters[18] and more polymerized aluminosilicate clusters[21] and is consistent with experimental observations.[38] Because the Si/Al distribution in the second coordination sphere as well as the Al−O−Al angle are expected to affect the δ_i^{Al} and δ_i^{Si}, these values may overlap for Si/Al of different Q^n speciations in complicated aluminosilicates. The δ_i^{Al} and δ_i^{Si} of the Si/Al (Q^1) in the Ca-linked dimers in general give somewhat smaller values (more shielded) than the corresponding dimers with similar T−O−T angles (Figure 7). This is consistent with the experimental observations that the interaction of cations affect the δ_i^{Al} and δ_i^{Si}, with higher field strength cations resulting in more shielded values.[38]

2.3. O(Al_3), O($SiAl_2$), O(Si_2Al), and O(Si)$_3$ Tricluster Oxygens. The ^{17}O QCC and the δ_i^O of the tricluster oxygens both increase in the order from O(Al^{IV}_3) (QCC = 3.0−3.3 MHz, δ_i^O = 38−40 ppm), to O($SiAl^{IV}_2$) (3.7−4.1 MHz, 47−48 ppm), to O(Si_2Al^{IV}) (5.0−5.2 MHz, 56−65 ppm), to O(Si_3) (6.2−6.4 MHz, 73−76 ppm) (see Figure 8). There are no experimental ^{17}O NMR data for tricluster oxygens in crystalline phases for direct comparison, although O(Al^{IV}_3) tricluster oxygen is present in a limited number of crystalline phases, such as the $CaAl_4O_7$ phase.[12] The calculated ^{17}O QCC of the O(Si^{IV}_3) tricluster oxygen is similar to the experimental value (6.5 MHz[39]) of O(Si^{VI}_3) (oxygen shared by three SiO_6 octahedra) in the high-pressure polymorph of SiO_2, stishovite, but its δ_i^O is smaller than the latter (109 ppm[39]). The calculated ^{17}O QCC of the O($SiAl^{IV}_2$) tricluster oxygen is close to that of O($SiAl^{IV}Al^V$) tricluster oxygen (3.2 MHz), but its δ_i^O is smaller than that of the latter (59 ppm). Thus, the present calculation and earlier experimental data both suggest that the ^{17}O QCC of tricluster oxygens is insensitive to the oxygen coordination number of the cations (Si or Al), but the δ_i^O is, with oxygens linked to higher coordination Si/Al, having a tendency to produce larger δ_i^O. The same trend is also exhibited by experimental ^{17}O NMR data for Si−O−Si BOs.[39] The consistency in the calculated values and experimental data could itself be regarded as a confidence test of the calculation.

Stebbins and Xu[3] have tentatively assigned a small feature (feature D estimated to have ^{17}O QCC of 2.3 MHz and δ_i^O of 20 ppm) in the ^{17}O 3Q MAS NMR spectrum of anorthite ($CaAl_2Si_2O_8$) glass to tricluster oxygens. However, none of the four types of tricluster oxygens we have calculated have as small δ_i^O and ^{17}O QCC as those of feature D. The calculated ^{17}O NMR parameters of the O(Al_3) and O($SiAl^{IV}_2$) triclusters overlap with those of Si−O−Al BOs (see Figure 8). The calculated ^{17}O QCC of the O(Si_2Al^{IV}) tricluster oxygens are similar to those of Si−O−Si BOs, their δ_i^O are somewhat larger than those of the latter

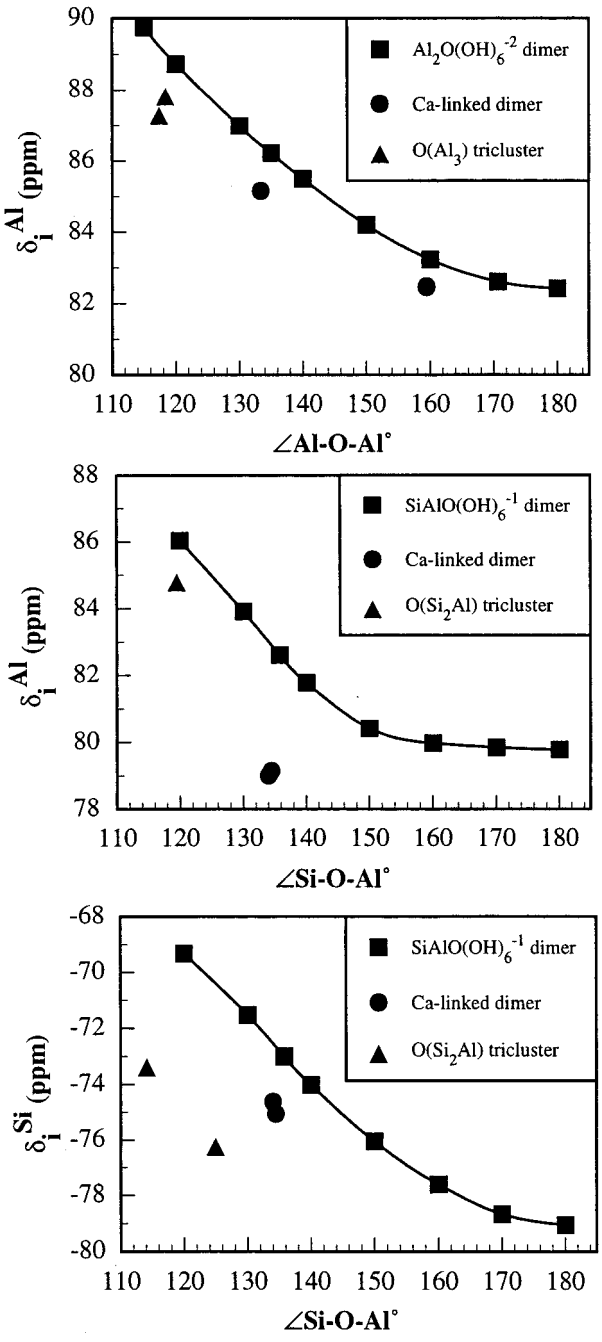

Figure 7. (Top) ^{27}Al isotropic chemical shifts (δ_i^{Al}) as a function of Al−O−Al angle for Al−O−Al linkage in $Al_2O(OH)_6^{2-}$ dimer, Al−O(Ca)−Al linkages in $Ca(Si_2O(OH)_6)(Al_2O(OH)_6)$ and $Ca(Al_2O(OH)_6)_2^{2-}$ Ca^{2+}-linked double dimer clusters, and $O(Al_3)$ tricluster in $Al_3O(OH)_9^{2-}$ and $SiAl_3O_3(OH)_9^{2-}$ clusters. (Middle and bottom) ^{27}Al and ^{29}Si isotropic chemical shifts (δ_i^{Al}, δ_i^{Al}) as a function of Si−O−Al angle for Si−O−Al linkage in $SiAlO(OH)_6^-$ dimer, Si−O(Ca)-Al linkages in $Ca(SiAlO(OH)_6)_2$ Ca^{2+}-linked double dimer, and $O(Si_2Al)$ tricluster in $Si_2AlO(OH)_9$ cluster. Only data for Al/Si (Q^1) are plotted. All calculated at HF/6-311+G(2df,p) (CSGT method) with HF/6-31+G-(d) geometries. Curves are spline fit to the data for the $Al_2O(OH)_6^{2-}$ or $SiAlO(OH)_6^-$ dimer.

(Figure 8). However, it is not unlikely that the δ_i^O of these two types of oxygen sites may actually overlap, because the experimental δ_i^O data for Si−O−Si BOs show a larger range of values than those calculated for small clusters. The overlap in structural parameters render it difficult to distinguish unambiguously, on the basis of ^{17}O NMR data alone, the $O(Al_3)$ or the $O(SiAl^{IV}_2)$ tricluster oxygens from Si−O−Al BOs and the $O(Si_2Al^{IV})$ tricluster oxygen from Si−O−Si BOs. This may

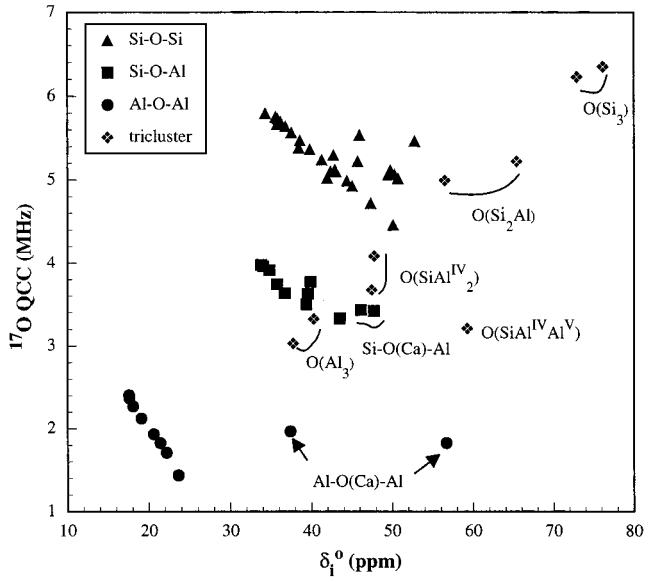

Figure 8. ^{17}O QCC as a function of ^{17}O chemical shift (δ_i^O) for different types of BOs and tricluster oxygens that are presented in Figures 4−6, all calculated at HF/6-311+G(2df,p) (CSGT method) with HF/6-31G(d) (for silicate clusters) or HF/6-31+G(d) (for aluminate and aluminosilicate clusters) geometries.

be particularly true for aluminosilicate glasses because peaks for each type of oxygen site are generally broad as a result of the disordered nature of glass structure (range of bond angles, bond lengths, different second nearest neighbors, etc.). It is of course entirely possible that these different types of oxygen sites give well-resolved ^{17}O NMR peaks for crystalline aluminosilicates. We would also like to note that our calculations suggest that it may be straightforward to distinguish the $O(Al_3)$ tricluster oxygen from Al−O−Al BO in aluminates using the ^{17}O NMR technique. The $O(Si_3)$ is the only type of tricluster oxygens that has ^{17}O NMR parameters sufficiently different from BOs in aluminosilicates and silicates, although its large ^{17}O QCC implies that it would be difficult to detect at small concentrations with the MQ MAS NMR technique.

The δ_i^{Al} of the Al^{IV} (Q^1 and Q^2) in all types of triclusters are in the range 78−88 ppm (Table 2), overlapping with those of Al^{IV} (Q^1) in $SiAlO(OH)_6^-$ dimers (80−86 ppm) and $Al_2O(OH)_6^{2-}$ dimers (82−89 ppm) and Al^{IV} (Q^2) in $Al_4O_4(OH)_8^{4-}$ and $Si_2Al_2O_4(OH)_8^{2-}$ four-membered ring clusters (77−81 ppm, see Table 2). The δ_i^{Si} of the Si^{IV} (Q^1 and Q^2) in these triclusters are in the range −70 to −86 ppm, overlapping with those of $Si^{IV}(Q^1)$ in $SiAlO(OH)_6^-$ dimers (−69 to −79 ppm) and $Si_2O(OH)_6$ dimers (Q^2, −74 to −84 ppm) and $Si^{IV}(Q^2)$ in $Si_2Al_2O_4(OH)_8^{2-}$ four-membered ring clusters (−77 − −80 ppm) (see Table 2). The range of δ_i^{Al} and δ_i^{Si} values of the triclusters is caused by several factors, including the proportion of Al in the tricluster, the degree of polymerizations (similar to Si(Al)−O−Si(Al) linkages) and the presence/absence of tetrahedral edge sharing. The δ_i^{Al} and δ_i^{Si} of the tricluster Al/Si seem to decrease with decreasing proportion of Al in the tricluster and decrease with increasing degree of polymerization (from Q^1 to Q^2). Tricluster Al/Si in more polymerized structures (Q^3 and Q^4) would probably yield even smaller chemical shift. Interestingly, the δ_i^{Al} and δ_i^{Si} of $O(Si,Al)_3$ tricluster are moderately smaller than those of corresponding Si(Al)−O−Si(Al) linkages (with the same polymerization, Q^n, and T−O−T angle), similar to those of the corresponding Si(Al)−O(Ca)−Si(Al) linkages (see examples plotted in Figure 7). Thus, in terms of δ_i^{Al} and δ_i^{Si}, the interaction of an extra Si^{IV} (or Al^{IV}) to a Si-

TABLE 3: Comparison of ^{29}Si, ^{27}Al, and ^{17}O Chemical Shifts Calculated at RHF/6-311+G(2df,p) (CSGT method) with Geometries Optimized at Different Levels of Theory[a]

	TOT angle (deg)			δ_i^{Si} (ppm)			δ_i^{Al} (ppm)			δ_i^{Ob} (ppm)		
cluster	1	2	3	1	2	3	1	2	3	1	2	3
$Si(OH)_4$				−73.8	−74.7	−73.7				16.7	16.9	12.2
$Si_2O(OH)_6$ dimer (C_2)	134.9	140.2	132.2	−79.4	−81.0	−78.5				42.9	43.0	36.5
$SiAlO(OH)_6^-$ dimer	135.8	137.3	133.4	−73.0	−73.5	−72.2	82.6	81.6	81.2	36.7	38.6	29.6
$Al_2O(OH)_6^{2-}$ dimer (C_2)	170.7	171.3	170.2				82.6	82.5	81.1	17.6	20.1	8.7
$Al_3O(OH)_6^{2-}$ tricluster (C_3)	118.4	118.6	117.8				87.8	86.7	86.8	40.3	41.2	32.6

[a] Geometry optimization method: (1) HF/6-31+G(d); (2) HF/6-311+G(2df,p); (3) B3LYP/6-311+G(2df,p). [b] For the dimers and tricluster, only data for the BOs and tricluster oxygens are presented.

TABLE 4: Comparison of ^{29}Si and ^{27}Al Chemical Shifts of Selected Clusters Calculated with Different Methods[a]

	δ_i^{Si} (ppm)				δ_i^{Al} (ppm)			
	HF		B3LYP		HF		B3LYP	
cluster	GIAO	CSGT	GIAO	CSGT	GIAO	CSGT	GIAO	CSGT
$Si(OH)_4$	−76.2	−73.7	−76.8	−75.9				
$Si_2O(OH)_6$ dimer (C_2)	−81.0	−78.5	−83.6	−82.2				
$SiAlO(OH)_6^-$ dimer	−74.3	−72.2	−74.4	−73.5	82.2	81.2	85.1	84.4
$Al_2O(OH)_6^{2-}$ dimer (C_2)					82.3	81.1	86.7	85.9
$Al_3O(OH)_6^{2-}$ tricluster (C_3)					88.3	86.8	92.7	91.4
	^{29}Si isotropic shidleing (ppm)				^{27}Al isotropic shielding (ppm)			
TMS	384.4	385.1	328.7	329.1				
$Al^{3+}(H_2O)_6$					613.7	610.4	574.8	572.3

[a] All geometries optimized at B3LYP/6-311+G(2df,p).

(Al)−O−Si(Al) linkage (to form a tricluster) is apparently similar to the interaction of a charge-balancing cation, such as Ca^{2+}. It should be noted that in these calculated clusters, only one of the four oxygens for each AlO_4 or SiO_4 tetrahedron within the tricluster is a tricluster oxygen. When coordinated to more than one tricluster oxygen, Al and Si would probably yield even smaller chemical shift. The experimental δ_i^{Al} data for the two tricluster Al sites (Q^4) in the crystalline $CaAl_4O_7$ phase that are each coordinated with one and two tricluster oxygens, respectively, have been reported to be 75.5 and 69.5 ppm,[40] in general agreement with our calculation.

In brief, our calculation for the small aluminosilicate clusters shows that the δ_i^{Al} or δ_i^{Si} of Al^{IV}/Si^{IV} (Q^1 and Q^2) in triclusters overlap with those not involved in triclusters, although the former tend to be smaller for a given polymerization, Q^n, and T−O−T angle. Thus, identification of triclusters in aluminosilicate glasses using ^{27}Al or ^{29}Si NMR may not be unique as well, although it is entirely possible that triclusters give well-resolved ^{27}Al or ^{29}Si NMR peaks for crystalline materials. Because unlike the ^{17}O NMR parameters, the δ_i^{Al} and δ_i^{Si} values of both Al^{IV}/Si^{IV} involved in triclusters and those not involved show significant dependence on the degree of polymerization, similar calculations for larger clusters would be necessary for quantitative conclusions for more polymerized structures (Q^3 and Q^4).

Finally, the δ_i^{Al} of the Al^V in the $Si^{IV}Al^{IV}Al^VO(OH)_9^-$ tricluster is 55.0 ppm, similar to that of Al^V in $Al(OH)_5^{2-}$ cluster (49.7 ppm).

3. Effect of Basis Set and Method on the Calculated NMR Parameters. To test whether the conclusions from section 2 hold at higher levels of theory, we have performed further calculations on representative clusters: $Si(OH)_4$ monomer (S_4 symmetry), $Si_2O(OH)_6$ dimer (C_2), $SiAlO(OH)_6^-$ dimer, $Al_2O(OH)_6^{2-}$ dimer (C_2), and $Al_3O(OH)_9^{2-}$ tricluster (C_3).

The first question is how much the basis set and method for geometry optimization affect the calculated NMR values. In Table 3, we compare the δ_i^{Si}, δ_i^{Al}, and δ_i^O values for these clusters calculated with the CSGT method at HF/6-311+G(2df,p) level on three different geometries optimized at HF/6-31+G(d), HF/6-311+G(2df,p), and B3LYP/6-311+G(2df,p) levels, respectively. The DFT methods are known to give superior geometries than the HF method.[30] The resultant δ_i^{Si}, δ_i^{Al}, and δ_i^O values are nearly the same (within 3 ppm) for the HF/6-31+G(d) and HF/6-311+G(2df,p) geometries. The δ_i^{Si} and δ_i^{Al} values of the B3LYP/6-311+G(2df,p) geometry are also nearly the same (within 2 ppm) as those of the HF geometries. The δ_i^O values of the B3LYP/6-311+G(2df,p) geometry are 5−11 ppm smaller than those of the HF geometries, although the relative differences in δ_i^O among these clusters are within 6 ppm of those of the HF geometries. Thus, from the NMR point of view, within the HF theory, optimization with the 6-31+G(d) basis set is as good as the 6-311+G(2df,p) basis set; optimization at B3LYP/6-311+G(2df,p) does not cause significant changes to the δ_i^{Si} and δ_i^{Al} values either and but does cause some change to the δ_i^O value.

The next issue is whether the employment of different methods (CSGT vs GIAO) for the NMR shielding calculations and different theories (HF vs DFT vs MP2) for the NMR shielding and EFG calculations would yield similar results. In Tables 4 and 5, we compare the δ_i^{Si}, δ_i^{Al}, and δ_i^O values, calculated with both the CSGT and the GIAO methods, and the ^{17}O QCC and EFG asymmetry η values, at HF/6-311+G(2df,p) and B3LYP/6-311+G(2df,p) levels. All these calculations were on cluster geometries optimized at B3LYP/6-311+G(2df,p). For the δ_i^{Si} and δ_i^{Al}, the GIAO and CSGT methods produce nearly identical results (within 2 ppm); the HF and B3LYP methods also yield similar results (within 5 ppm), although the GIAO method tends to give slightly less shielded values (larger chemical shift) than the CSGT method; and the B3LYP method gives somewhat less shielded values than the HF method. For the ^{17}O QCC and EFG asymmetry parameter η, both the HF and B3LYP methods give nearly identical values (QCC within 0.1 MHz, η within 0.1). The δ_i^O values show the largest variations. The GIAO method produces consistently larger δ_i^O values (by 14−21 ppm) than the CSGT method. This is mainly because the GIAO method yields a 15−

TABLE 5: Comparison of ^{17}O Chemical Shift and ^{17}O EFG Parameters of Selected Clusters Calculated with Different Methods[a]

	δ_i^{O}[b] (ppm)					^{17}O EFG parameters§			
	HF		B3LYP		MP2	HF		B3LYP	
cluster	GIAO	CSGT	GIAO	CSGT	GIAO	|QCC|* (MHz)	η	|QCC|[c] (MHz)	η
$Si(OH)_4$	25.9	12.2	41.7	26.6	38.6	8.06	0.47	8.05	0.48
$Si_2O(OH)_6$ dimer (C_2)	57.9	36.5	87.5	64.6		4.96	0.46	5.04	0.45
$SiAlO(OH)_6^-$ dimer	49.5	29.6	77.4	56.1		3.57	0.16	3.66	0.16
$Al_2O(OH)_6^{2-}$ dimer (C_2)	26.8	8.7	48.4	28.3		2.35	0.08	2.48	0.04
$Al_3O(OH)_6^{2-}$ tricluster (C_3)	48.2	32.6	86.1	68.6		3.11	0.00	3.21	0.00
	^{17}O isotropic shielding (ppm)					eq_{zz} (au)	η	eq_{zz} (au)	η
H_2O	325.4	310.4	324.0	308.4	344.6	1.8313	0.82	1.7747	0.79

[a] All geometries optimized at B3LYP/6-311+G(2df,p). [b] For the dimers and tricluster, only data for the BOs and tricluster oxygens are presented. [c] Absolute value.

16 ppm larger ^{17}O shielding value than the CSGT method for H_2O, the ^{17}O chemical shift standard. It turns out that the former value is closer to those calculated with much larger basis sets at which level the shielding values produced by the two methods converge. For example, the ^{17}O shielding values for H_2O calculated with the GIAO and CSGT methods at HF/6-311+G-(2df,p) are 325.4 and 310.4 ppm, respectively (see Table 5); the former is close to those calculated with the much larger basis AUG-cc-pV5Z using either method (GIAO, 324.0 ppm; CSGT, 324.1 ppm). Thus, for the δ_i^O values of aluminosilicates described here, those calculated using the GIAO method seem to be more reliable. Nevertheless, the relative differences among the δ_i^O values of the aluminosilicate clusters would change by only ≤ 5 ppm if the GIAO method, instead of the CSGT method, were adopted. Thus, the use of GIAO method would not change the conclusion from section 2. The B3LYP method gives consistently larger δ_i^O values than the HF method (by 15−38 ppm). Because no current functionals of the DFT methods adopted in Gaussian 98 include a magnetic field dependence, there is no guarantee that the DFT methods provide better NMR results than the HF method.[23] We have performed MP2 NMR calculations for only one cluster $Si(OH)_4$. The resultant δ_i^O value is close to that of the B3LYP calculation (see Table 5), suggesting that the B3LYP results for δ_i^O of aluminosilicates might be more reliable than the HF results, although more test is needed before a solid conclusion can be reached. Finally, it should be mentioned that because of the apparent large medium effect, the absolute values for δ_i^O of small aluminosilicate clusters (that are more representative of gaseous phases) do not necessarily agree with those of condensed aluminosillicates, although the relative values among these clusters are likely to be applicable to the latter.

In summary, the calculated δ_i^{Si} and δ_i^{Al} values are insensitive (within a few ppm) to the basis set and method of calculations above HF/6-311+G(2df,p)//HF/6-31+G(d) (method and basis set for NMR and EFG calculation//method and basis set for geometry optimization) that is adopted in section 2. The relative order of the δ_i^O of representative aluminosilicate clusters are also essentially the same with either the CSGT or the GIAO method, the HF or the B3LYP theory, for either geometry optimization or NMR calculations: the Si−O−Si BO of the $Si_2O(OH)_6$ dimer (C_2) gives slightly larger δ_i^O than the Si−O−Al BO of the $SiAlO(OH)_6^-$ dimer; the Al−O−Al BO of the $Al_2O(OH)_6^{2-}$ dimer (C_2) gives much smaller δ_i^O than the Si−O−Si BO or the Si−O−Al BO; the $O(Al_3)$ tricluster oxygen of $Al_3O(OH)_6^{2-}$ tricluster gives δ_i^O similar to those of the Si−O−Si and Si−O−Al BOs and larger than that of Al−O−Al BO. The calculated ^{17}O QCC and EFG asymmetry η values are even less sensitive to the theory and basis set of calculations (within 0.1 MHz and 0.1, respectively, of one another). Thus, the conclusions from section 2 would not be affected.

4. Implications to the Structure of Aluminosilicate Glasses. Our calculations suggest that the Al−O−Al, Si−O−Al, and Si−O−Si BOs produce progressively larger ^{17}O QCC values and larger, but overlapping, δ_i^O. Identification of these different types of BOs may thus be straightforward. It may be difficult to distinguish $O(Al_3)$ and $O(SiAl_2)$ tricluster oxygens from Si−O−Al BOs or to distinguish the $O(Si_2Al)$ tricluster oxygen from Si−O−Si BOs on the basis of ^{17}O NMR data alone. The $O(Si_3)$ triclusters have larger δ_i^O and ^{17}O QCC than all types of BOs. Thus, in principle, it is possible to distinguish the $O(Si_3)$ tricluster oxygen from the other types of oxygen sites, although its large ^{17}O QCC implies that it is difficult to detect small amounts of such tricluster oxygens.

These calculation results should be helpful in interpreting experimental ^{17}O 3Q MAS NMR data for aluminosilicate glasses. Dirken et al.[6] showed for an albite glass that there are two well-separated contours that can be assigned to Si−O−Al BO (^{17}O QCC = 3.5 MHz; δ_i^O = 33 ppm) and Si−O−Si BO (5.1 MHz; 49 ppm), respectively. There are no detectable features in the spectra due to Al−O−Al BOs or other oxygen sites. Stebbins and Xu[3] showed for an anorthite glass that the main feature (3.5 MHz; 61 ppm) can be attributed to Si−O−Al BO and a smaller overlapping feature (5.5 MHz; 50 ppm) can be assigned to Si−O−Si BO. The highlight of their study was to demonstrate that there is a small feature (2.9 MHz; 113 ppm) that can only be attributed to NBO. This was a significant observation because glasses of tectosilicate compositions have been assumed to be fully polymerized thus far. The detection of NBOs would change our view about the physical properties, such as viscosities, of melts and glasses in such systems, because of the important role NBO plays in the viscous processes. The appearance of NBOs in such system, in the absence of higher coordination Si or Al, would require the concurrent presence of other oxygen sites that are coordinated to more than two tetrahedral cations (Si or Al). They have assigned a small feature (feature D: 2.3 MHz, 20 ppm) to tricluster oxygens. Our calculation supports the assignment of Si−O−Si and Si−O−Al BOs of both studies. However, our result does not agree with the assignment by Stebbins and Xu[3] of feature D to tricluster oxygens. This feature rather resembles Al−O−Al BOs. Therefore, if the small feature D is real, it may be an indication that a small amount of Al−O−Al BOs is present in the anorthite glass of Stebbins and Xu.[3] Our calculations show that even if tricluster oxygens are present in the aluminosilicate glass structure, it may be either difficult to distinguish them from Si−O−Al BOs (in the case of $O(Al_3)$ and $O(SiAl_2)$ tricluster oxygens) or Si−O−Si BO (in the case of $O(Si_2Al)$ tricluster

oxygen) or the peaks may be too broad to allow detection at small concentrations (in the case of $O(Si_3)$ tricluster oxygen).

Finally, it should be noted that in contrast to aluminosilicates, ^{17}O NMR should be a useful tool for identification of triclusters in aluminates, because there is only one possible type of BO (Al−O−Al) and one type of tricluster oxygen ($O(Al_3)$) in the latter, each with distinct ^{17}O QCC.

Acknowledgment. We thank J. F. Stebbins and an anonymous reviewer for helpful comments. We would also like to acknowledge the Molecular Science Computing Facility, Environmental and Molecular Sciences Laboratory for making available the basis sets for Ca in the Extensible Computational Chemistry Environment Basis Set Database. The cluster structures are plotted using the PPC_MacMolplt software by Brett Bode. The calculations were mostly performed on a HP Exemplar V2250, funded by the Ministry of Education, Science, Sports and Culture of Japan.

References and Notes

(1) Mysen, B. O. *Structure and Properties of Silicate Melts*; Elsevier: Amsterdam, 1988; Vol. 4.

(2) Toplis, M. J.; Dingwell, D. B.; Lenci, T. *Geochim. Cosmochim. Acta* **1997**, *61*, 2605.

(3) Stebbins, J. F.; Xu, Z. *Science* **1997**, *390*, 60.

(4) Lacy, E. D. *Phys. Chem. Glasses* **1963**, *4*, 234.

(5) Lowenstein, W. *Am. Mineral.* **1954**, *39*, 92.

(6) Dirken, P. J.; Kohn, S. C.; Smith, M. E.; van Eck, E. R. H. *Chem. Phys. Lett.* **1997**, *266*, 568.

(7) Stebbins, J. F.; Lee, S. K.; Oglesby, J. V. *Am. Mineral.* **1999**, *84*, 983.

(8) Grandinetti, P. J.; Baltisberger, J. H.; Farnan, I.; Stebbins, J. F.; Werner, U.; Pines, A. *J. Phys. Chem.* **1995**, *99*, 12341.

(9) Bull, L. M.; Cheetham, A. K.; Anupold, T.; Reinhold, A.; Samoson, A.; Sauer, J.; Bussemer, B.; Lee, Y.; Gann, S.; Shore, J.; Pines, A.; Dupree, R. *J. Am. Chem. Soc.* **1998**, *120*, 3510.

(10) Xu, Z.; Stebbins, J. F. *Solid State Nucl. Magn. Reson.* **1998**, *11*, 243.

(11) Pingel, U.-T.; Amoureux, J.-P.; Anupold, T.; Bauer, F.; Ernst, H.; Fernandez, C.; Freude, D.; Samoson, A. *Chem. Phys. Lett.* **1998**, *294*, 345.

(12) Goodwin, D. W.; Lindop, A. J. *Acta Crystallogr.* **1970**, *B26*, 1230.

(13) Tossell, J. A.; Lazzeretti, P. *Chem. Phys.* **1987**, *112*, 205.

(14) Tossell, J. A.; Lazzeretti, P. *Phys. Chem. Miner.* **1988**, *15*, 564.

(15) Tossell, J. A. *J. Non-Cryst. Solids* **1990**, *120*, 13.

(16) Tossell, J. A. *Am. Mineral.* **1993**, *78*, 911.

(17) Farnan, I.; Grandinetti, P. J.; Baltisberger, J. H.; Stebbins, J. F.; Werner, U.; Eastman, M. A.; Pines, A. *Nature* **1992**, *358*, 31.

(18) Xue, X.; Kanzaki, M. *Phys. Chem. Miner.* **1998**, *26*, 14.

(19) Moravetski, V.; J. R.; H.; Eichler, U.; Cheetham, A. K.; Sauer, J. *J. Am. Chem. Soc.* **1996**, *118*, 13015.

(20) Tossell, J. A.; Sághi-Szabó, G. *Geochim. Cosmochim. Acta* **1997**, *61*, 1171.

(21) Sykes, D.; Kubicki, J. D.; Farrar, T. C. *J. Phys. Chem.* **1997**, *101*, 2715.

(22) Tossell, J. A. *J. Magn. Reson.* **1997**, *127*, 49.

(23) Frisch, M. J.; Trucks, G. W.; Schlegel, H. B.; Scuseria, G. E.; Robb, M. A.; Cheeseman, J. R.; Zakrzewski, V. G.; Montgomery, J. A.; Stratmann, R. E.; Burant, J. C.; Dapprich, S.; Millam, J. M.; Daniels, A. D.; Kudin, K. N.; Strain, M. C.; Farkas, O.; Tomasi, J.; Barone, V.; Cossi, M.; Cammi, R.; Mennucci, B.; Pomelli, C.; Adamo, C.; Clifford, S.; Ochterski, J.; Petersson, G. A.; Ayala, P. Y.; Cui, Q.; Morokuma, K.; Malick, D. K.; Rabuck, A. D.; Raghavachari, K.; Foresman, J. B.; Cioslowski, J.; Ortiz, J. V.; Stefanov, B. B.; Liu, G.; Liashenko, A.; Piskorz, P.; Komaromi, I.; Gomperts, R.; Martin, R. L.; Fox, D. J.; Keith, T.; Al-Laham, M. A.; Peng, C. Y.; Nanayakkara, A.; Gonzalez, C.; Challacombe, M.; Gill, P. M. W.; Johnson, B.; Chen, W.; Wong, M. W.; Andres, J. L.; Gonzalez, C.; Head-Gordon, M.; Replogle, E. S.; Pople, J. A. *Gaussian 98*, revision A.3; Gaussian, Inc.: Pittsburgh, PA, 1998.

(24) Keith, T. A.; Bader, R. F. W. *Chem. Phys. Lett.* **1993**, *210*, 223.

(25) Rassolov, V. A.; Pople, J. A.; Ratner, M. A.; Windus, T. L. *J. Chem. Phys.* **1998**, *109*, 1223.

(26) Blaudeau, J.-P.; McGrath, M. P.; Curtiss, L. A.; Radom, L. *J. Chem. Phys.* **1997**, *107*, 5016.

(27) Kanzaki, M. *Mineral. J.* **1996**, *18*, 1.

(28) Kanzaki, M. *J. Ceram. Soc. Jpn.* **1997**, *105*, 91.

(29) Verhoeven, J.; Dymanus, A.; Bluyssen, H. *J. Chem. Phys.* **1969**, *15*, 3330.

(30) Foresman, J. B.; Frisch, Æ. *Exploring chemistry with electronic structure methods*; Gaussian, Inc.: Pittsburgh, PA, 1996.

(31) Cheeseman, J. R.; Trucks, G. W.; Keith, T. A.; Frisch, M. J. *J. Chem. Phys.* **1996**, *104*, 5497.

(32) Wainwright, J. E.; Starkey, J. *Z. Kristallogr.* **1971**, *133*, 75.

(33) Johansson, G. *Acta Chem. Scand.* **1966**, *20*, 505.

(34) Hörkner, W.; Müller-Buschbaum, H. K. *J. Inorg. Nucl. Chem.* **1976**, *38*, 983.

(35) Spearing, D. R.; Farnan, I.; Stebbins, J. F. *Phys. Chem. Miner.* **1992**, *19*, 307.

(36) Vermillion, K. E.; Florian, P.; Grandinetti, P. J. *J. Chem. Phys.* **1998**, *108*, 7274.

(37) Timken, H. K. C.; Schramm, S. E.; Kirkpatrick, R. J.; Oldfield, E. *J. Phys. Chem.* **1987**, *91*, 1054.

(38) Stebbins, J. F. Nuclear magnetic resonance spectroscopy of silicates and oxides in geochemistry and geophysics. In *Mineral Physics & Crystallography, A Handbook of Physical Constants*; Ahrens, T. J., Ed.; The American Geophysical Union: Washington, DC, 1995; p 303.

(39) Xue, X.; Stebbins, J. F.; Kanzaki, M. *Am. Mineral.* **1994**, *79*, 31.

(40) Skibsted, J.; Henderson, E.; Jakobsen, H. J. *Inorg. Chem.* **1993**, *32*, 1013.